

Supplement of Geosci. Model Dev., 13, 5175–5190, 2020
<https://doi.org/10.5194/gmd-13-5175-2020-supplement>
© Author(s) 2020. This work is distributed under
the Creative Commons Attribution 4.0 License.



Supplement of

Reduced Complexity Model Intercomparison Project Phase 1: introduction and evaluation of global-mean temperature response

Zebedee R. J. Nicholls et al.

Correspondence to: Zebedee Nicholls (zebedee.nicholls@climate-energy-college.org)

The copyright of individual parts of the supplement might differ from the CC BY 4.0 License.

S1 Data formats

Systematic intercomparison projects such as RCMIP require the definition of a clear input and output data handling framework. Historically, comparing RCMs required learning how to set up, configure and run multiple RCMs in order to produce results. This required significant time and hence, as previously discussed, has only been attempted in standalone cases with a limited number of models (Houghton et al., 1997; van Vuuren et al., 2011; Harmsen et al., 2015; Schwarber et al., 2019). With a common framework, once a model has participated in RCMIP, it is simpler to run it again in different experiments and provide output in a common, standardised format. This allows researchers to design, run and analyse experiments with far less effort than was previously required. As a result, it becomes feasible to do more regular and targeted assessment of RCMs. This capacity improves our knowledge of RCMs, our understanding of the implications of their quantitative results and our ability to develop and improve them. Our data format is designed to be easy to use and hence easily able to be extended within future RCMIP phases or in separate research.

S1.1 Inputs

All input data is provided in a text-based format based on the specifications used by the IAMC community (Gidden and Huppmann, 2019). The computational simplicity of RCMs means that their input specifications are relatively lightweight and hence using an uncompressed, text-based input format is possible. Further, the format is explicit about associated metadata and ensures metadata remains attached to the timeseries. As the IAMC community is a major user of RCMs, as well as being the source of input data for many experiments run with RCMs, using their data format ensures that data can be shared easily and assessment of IAM emissions scenarios can be performed with minimal data handling overhead.

The inputs are formatted as text files with comma separated values (CSV), with each row of the CSV file being a timeseries (see rcmip.org). This format is also often referred to as ‘wide’ although this term is imprecise (Wickham, 2014). The columns provide metadata about the timeseries, specifically the timeseries’ variable, units, region, model and scenario. Other columns provide the values for each timestep within the timeseries.

Being simplified models, RCMs typically do not take gridded input. Hence we use a selection of highly aggregated socio-economic regions, which once again follow IAMC conventions (Gidden and Huppmann, 2019).

25 S1.2 Outputs

RCMIP Phase 1’s submission template (see rcmip.org or <https://doi.org/10.5281/zenodo.3593570>) is composed of two parts. The first part is the data submission and is identical to the input format. Using a consistent data format allows for simplified analysis with the same tools we used to develop the input protocols and exchange with the IAMC community as they can analyse the data using existing tools such as pyam (Gidden and Huppmann, 2019). However, one complication of using the IAMC format is that the ‘model’ column is reserved for the name of the integrated assessment model which produced the scenario. To enhance compatibility with the IAMC format, we don’t use the ‘model’ column. Instead, we use the separate ‘climate_model’ column to store metadata about the climate model which provided the timeseries.

The second part of submissions is model metadata. This includes the model's name, version number, brief description and literature reference. We also request a configuration label, which uniquely identifies the configuration in which the model was
35 run to produce the given results.

Given the typical temporal resolution of RCMs, we request all output be reported with an annual timestep. In addition, to facilitate use of the output, participating modelling groups agree to have their submitted data made available under a Creative Commons Attribution-ShareAlike 4.0 International (CC BY-SA 4.0) license. All input and output data, as well as all code required to produce this paper, is available at gitlab.com/rcmip/rcmip and archived at <https://doi.org/10.5281/zenodo.3593569>.

40 S2 Scenario-based experiments data sources

CMIP6 emissions projections follow Gidden et al. (2019) and are available at <https://tntcat.iiasa.ac.at/SspDb/dsd?Action=htmlpage&page=60> (hosted by IIASA). Where regional emissions information is missing, we use the downscaling procedure described in Meinshausen et al. (2020). The emissions extensions also follow the convention described in Meinshausen et al. (2020).

45 For CMIP6 historical emissions (year 1850-2014), we have used data sources which match the harmonisation used for the CMIP6 emissions projections. This ensures consistency with CMIP6, although it means that we do not always use the latest data sources. CMIP6 historical anthropogenic emissions for CO₂, CH₄, BC, CO, NH₃, NOx, OC, SO₂ and non-methane volatile organic compounds (NMVOCs) come from CEDS (Hoesly et al., 2018). Biomass burning emissions data for CH₄, BC, CO, NH₃, NOx, OC, SO₂ and NMVOCs come from UVA (van Marle et al., 2017). The biomass burning emissions are
50 a blend of both anthropogenic and natural emissions, which could lead to some inconsistency between RCMs as they make different assumptions about the particular anthropogenic/natural emissions split. CO₂ global land-use emissions are taken from the Global Carbon Budget 2016 (Quéré et al., 2016). Emissions of N₂O and the regional breakdown of CO₂ land-use emissions come from PRIMAP-hist Version 1.0 (Gütschow et al., 2016, see <https://doi.org/10.5880/PIK.2016.003>). Where well-mixed greenhouse gas emissions are missing, we use inverse emissions based on the CMIP6 concentrations from MAGICC7.0.0
55 (Meinshausen et al., 2020). Where required, historical emissions were extended back to 1750 by assuming a constant relative rate of decline based on the period 1850-1860 (noting that historical emissions are somewhat uncertain, we require consistent emissions inputs in Phase 1, uncertainty in historical emissions will be explored in future research).

CMIP6 concentrations follow Meinshausen et al. (2020). CMIP6 radiative forcings follow the data provided at <https://doi.org/10.5281/zenodo.3515339>. CMIP5 emissions, concentrations and radiative forcings follow Meinshausen et al. (2011) and
60 are taken from <http://www.pik-potsdam.de/~mmalte/rcps/>.

Table S1. Emulation scores and equilibrium climate sensitivities (ECSs) for RCMIP model calibrations. In parentheses we show the number of simulations available for each model variant.

| Target CMIP6 model | RCMIP model | RMSE (K) |
|----------------------------|-------------------------|----------|
| AWI-CM-1-1-MR_r1i1p1f1 (5) | MAGICC-v7-1-0-beta (5) | 0.16 |
| BCC-CSM2-MR_r1i1p1f1 (6) | MCE-v1-1 (2) | 0.21 |
| | MAGICC-v7-1-0-beta (6) | 0.16 |
| | ar5ir-2box (2) | 0.13 |
| | ar5ir-3box (2) | 0.13 |
| | held-two-layer-uom (2) | 0.13 |
| BCC-ESM1_r1i1p1f1 (4) | MCE-v1-1 (2) | 0.12 |
| | MAGICC-v7-1-0-beta (3) | 0.13 |
| | ar5ir-2box (2) | 0.18 |
| | ar5ir-3box (2) | 0.15 |
| | held-two-layer-uom (2) | 0.12 |
| CanESM5_r1i1p1f1 (10) | MCE-v1-1 (2) | 0.13 |
| | hector (9) | 0.18 |
| | MAGICC-v7-1-0-beta (10) | 0.30 |
| | ar5ir-2box (2) | 0.19 |
| | ar5ir-3box (2) | 0.21 |
| | held-two-layer-uom (2) | 0.30 |
| CanESM5_r1i1p2f1 (7) | MCE-v1-1 (2) | 0.13 |
| | hector (7) | 0.18 |
| | MAGICC-v7-1-0-beta (7) | 0.27 |
| CanESM5_r10i1p1f1 (5) | hector (5) | 0.22 |
| | MAGICC-v7-1-0-beta (5) | 0.18 |
| CESM2-WACCM_r1i1p1f1 (6) | MCE-v1-1 (2) | 0.15 |
| | hector (6) | 0.22 |
| | MAGICC-v7-1-0-beta (6) | 0.21 |
| | ar5ir-2box (2) | 0.45 |
| | ar5ir-3box (2) | 0.21 |
| | held-two-layer-uom (2) | 0.13 |

Table S1. Continued.

| Target CMIP6 model | RCMIP model | RMSE (K) |
|----------------------------|------------------------|----------|
| | | |
| CESM2_r1i1p1f1 (6) | MCE-v1-1 (2) | 0.17 |
| | hector (6) | 0.32 |
| | MAGICC-v7-1-0-beta (6) | 0.27 |
| | ar5ir-2box (2) | 0.24 |
| | ar5ir-3box (2) | 0.24 |
| | held-two-layer-uom (2) | 0.20 |
| CNRM-CM6-1_r1i1p1f2 (8) | MCE-v1-1 (4) | 0.24 |
| | hector (8) | 0.34 |
| | MAGICC-v7-1-0-beta (8) | 0.18 |
| | ar5ir-2box (4) | 0.43 |
| | ar5ir-3box (4) | 0.43 |
| | held-two-layer-uom (4) | 0.16 |
| CNRM-ESM2-1_r1i1p1f2 (10) | MCE-v1-1 (2) | 0.20 |
| | hector (9) | 0.24 |
| | MAGICC-v7-1-0-beta (9) | 0.18 |
| | ar5ir-3box (2) | 0.27 |
| | ar5ir-2box (2) | 0.27 |
| | held-two-layer-uom (2) | 0.17 |
| E3SM-1-0_r1i1p1f1 (2) | MCE-v1-1 (2) | 0.17 |
| | MAGICC-v7-1-0-beta (2) | 0.22 |
| EC-Earth3-Veg_r1i1p1f1 (7) | MCE-v1-1 (2) | 0.19 |
| | MAGICC-v7-1-0-beta (7) | 0.25 |
| | ar5ir-3box (2) | 0.22 |
| | ar5ir-2box (2) | 0.27 |
| | held-two-layer-uom (2) | 0.19 |

Table S1. Continued.

| Target CMIP6 model | RCMIP model | RMSE (K) |
|----------------------------|------------------------|-----------------|
| FGOALS-g3_r1i1p1f1 (4) | MAGICC-v7-1-0-beta (4) | 0.15 |
| GISS-E2-1-G_r1i1p1f1 (4) | MCE-v1-1 (4) | 0.16 |
| | MAGICC-v7-1-0-beta (4) | 0.19 |
| | ar5ir-2box (4) | 0.15 |
| | ar5ir-3box (4) | 0.58 |
| | held-two-layer-uom (4) | 0.15 |
| GISS-E2-1-H_r1i1p1f1 (3) | MCE-v1-1 (3) | 0.15 |
| | MAGICC-v7-1-0-beta (3) | 0.16 |
| | ar5ir-3box (3) | 0.15 |
| | ar5ir-2box (3) | 0.16 |
| | held-two-layer-uom (3) | 0.14 |
| GISS-E2-2-G_r1i1p1f1 (3) | MAGICC-v7-1-0-beta (3) | 0.19 |
| | ar5ir-3box (3) | 0.66 |
| | ar5ir-2box (3) | 0.16 |
| | held-two-layer-uom (3) | 0.14 |
| IPSL-CM6A-LR_r1i1p1f1 (20) | MCE-v1-1 (4) | 0.25 |
| | hector (9) | 0.40 |
| | MAGICC-v7-1-0-beta (9) | 0.25 |
| | ar5ir-2box (4) | 0.34 |
| | ar5ir-3box (4) | 0.26 |
| | held-two-layer-uom (4) | 0.29 |
| IPSL-CM6A-LR_r1i1p1f2 (2) | hector (2) | 0.34 |
| | MAGICC-v7-1-0-beta (2) | 0.21 |
| IPSL-CM6A-LR_r10i1p1f1 (3) | MCE-v1-1 (1) | 0.21 |
| | hector (3) | 0.34 |
| | MAGICC-v7-1-0-beta (3) | 0.32 |
| MCM-UA-1-0_r1i1p1f2 (4) | MAGICC-v7-1-0-beta (4) | 0.16 |

Table S1. Continued.

| Target CMIP6 model | RCMIP model | RMSE (K) |
|--------------------------|-------------------------|----------|
| MIROC6_r1i1p1f1 (14) | MCE-v1-1 (4) | 0.28 |
| | MAGICC-v7-1-0-beta (12) | 0.19 |
| NorESM2-LM_r1i1p1f1 (3) | MCE-v1-1 (2) | 0.32 |
| | MAGICC-v7-1-0-beta (2) | 0.22 |
| | ar5ir-3box (2) | 0.19 |
| | ar5ir-2box (2) | 0.19 |
| SAM0-UNICON_r1i1p1f1 (2) | MCE-v1-1 (2) | 0.15 |
| | MAGICC-v7-1-0-beta (2) | 0.24 |
| UKESM1-0-LL_r1i1p1f2 (9) | MCE-v1-1 (2) | 0.16 |
| | MAGICC-v7-1-0-beta (9) | 0.30 |
| | ar5ir-3box (2) | 0.19 |
| | ar5ir-2box (2) | 0.26 |
| | held-two-layer-uom (2) | 0.19 |

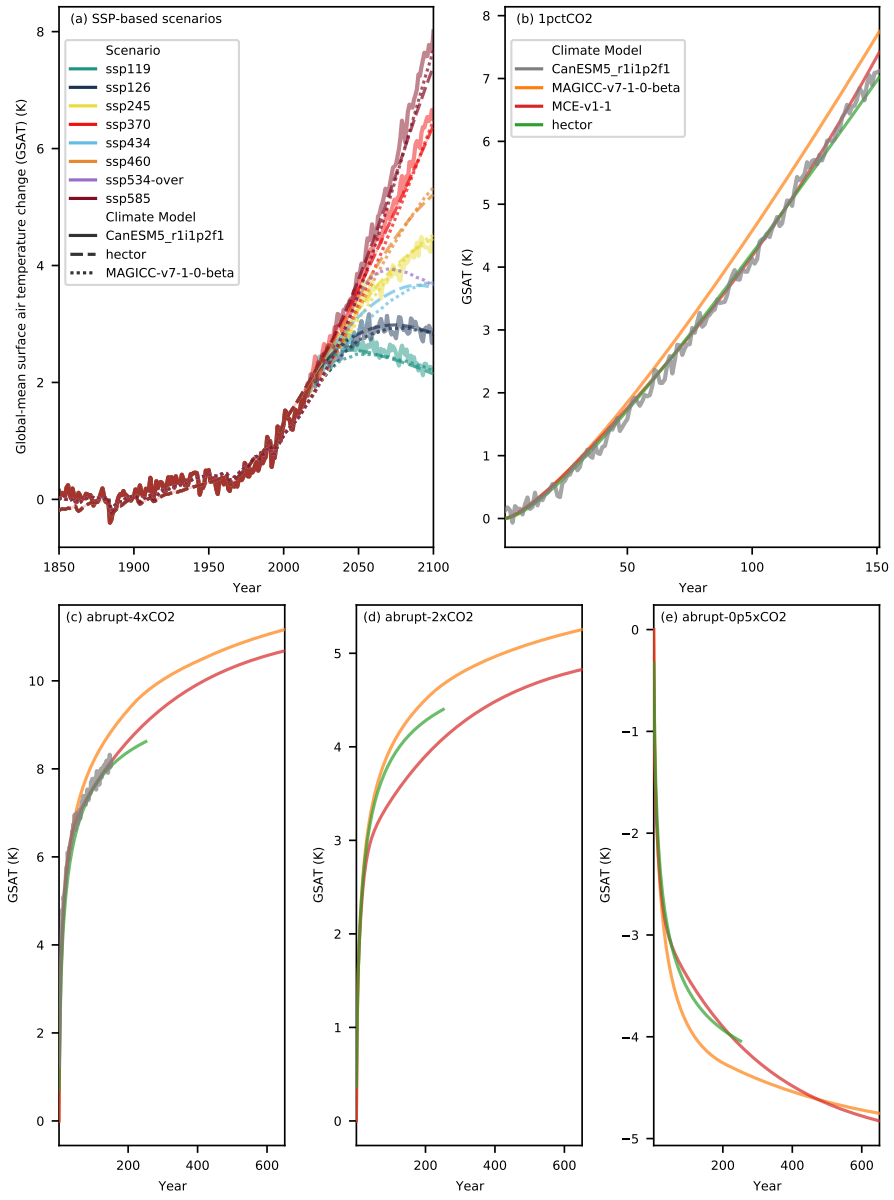


Figure S1. Emulation of CanESM5_r1i1p2f1 by RCMs in RCMIP Phase 1. The thick transparent lines are the target CMIP6 model output (here from CanESM5_r1i1p2f1). The thin lines are emulations from different RCMs. Panel (a) shows results for scenario based experiments while panels (b) - (e) show results for idealised CO₂-only experiments (note that panels (b) - (e) share the same legend).

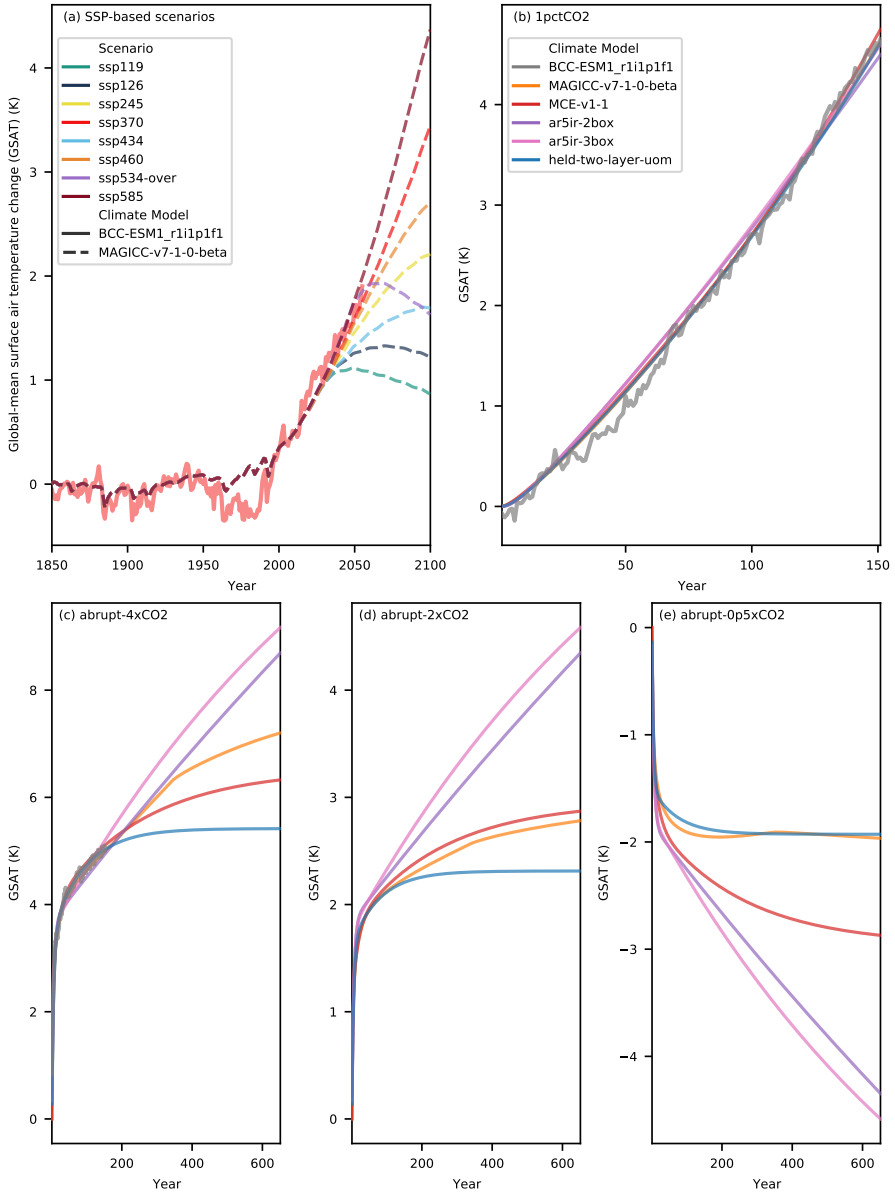


Figure S2. Emulation of BCC-ESM1_r1i1p1f1 by RCMs in RCMIP Phase 1. The thick transparent lines are the target CMIP6 model output (here from BCC-ESM1_r1i1p1f1). The thin lines are emulations from different RCMs. Panel (a) shows results for scenario based experiments while panels (b) - (e) show results for idealised CO₂-only experiments (note that panels (b) - (e) share the same legend).

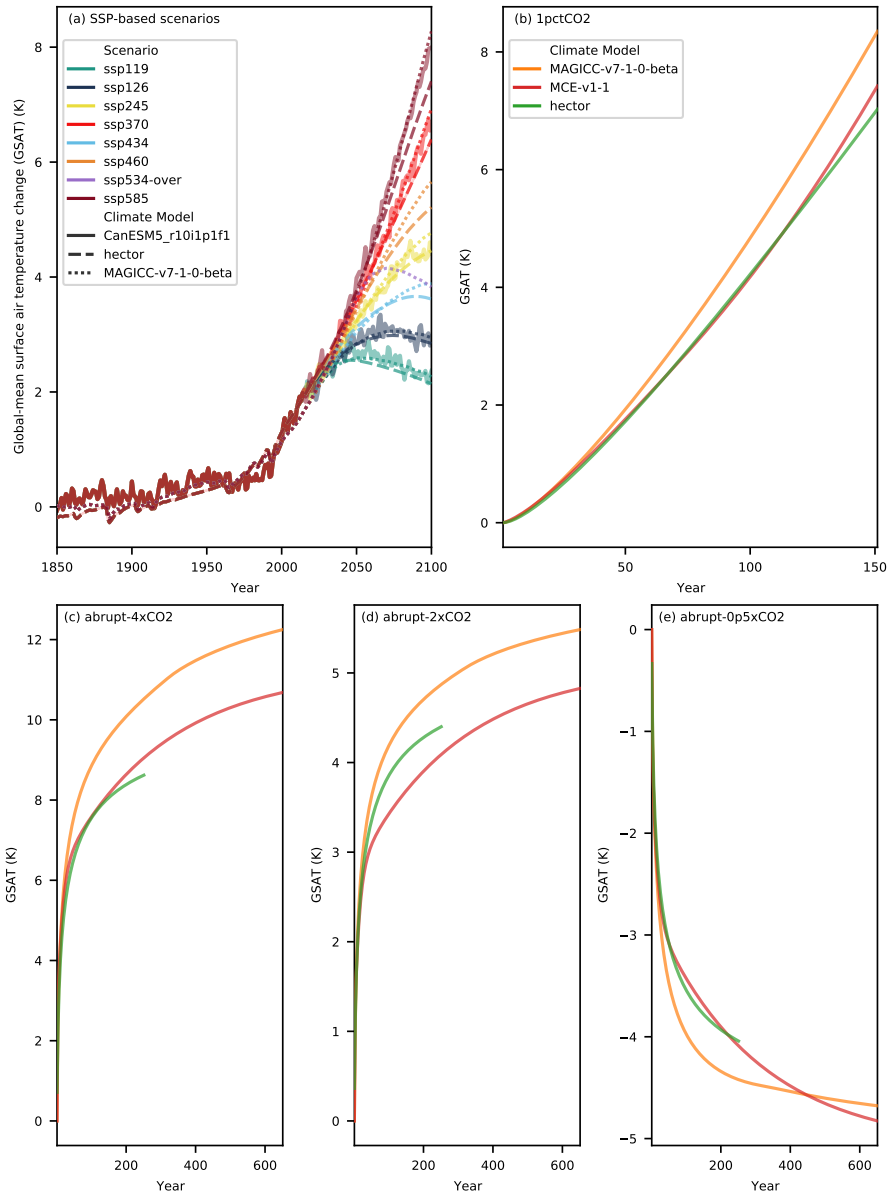


Figure S3. Emulation of CanESM5_r10i1p1f1 by RCMs in RCMIP Phase 1. The thick transparent lines are the target CMIP6 model output (here from CanESM5_r10i1p1f1). The thin lines are emulations from different RCMs. Panel (a) shows results for scenario based experiments while panels (b) - (e) show results for idealised CO₂-only experiments (note that panels (b) - (e) share the same legend).

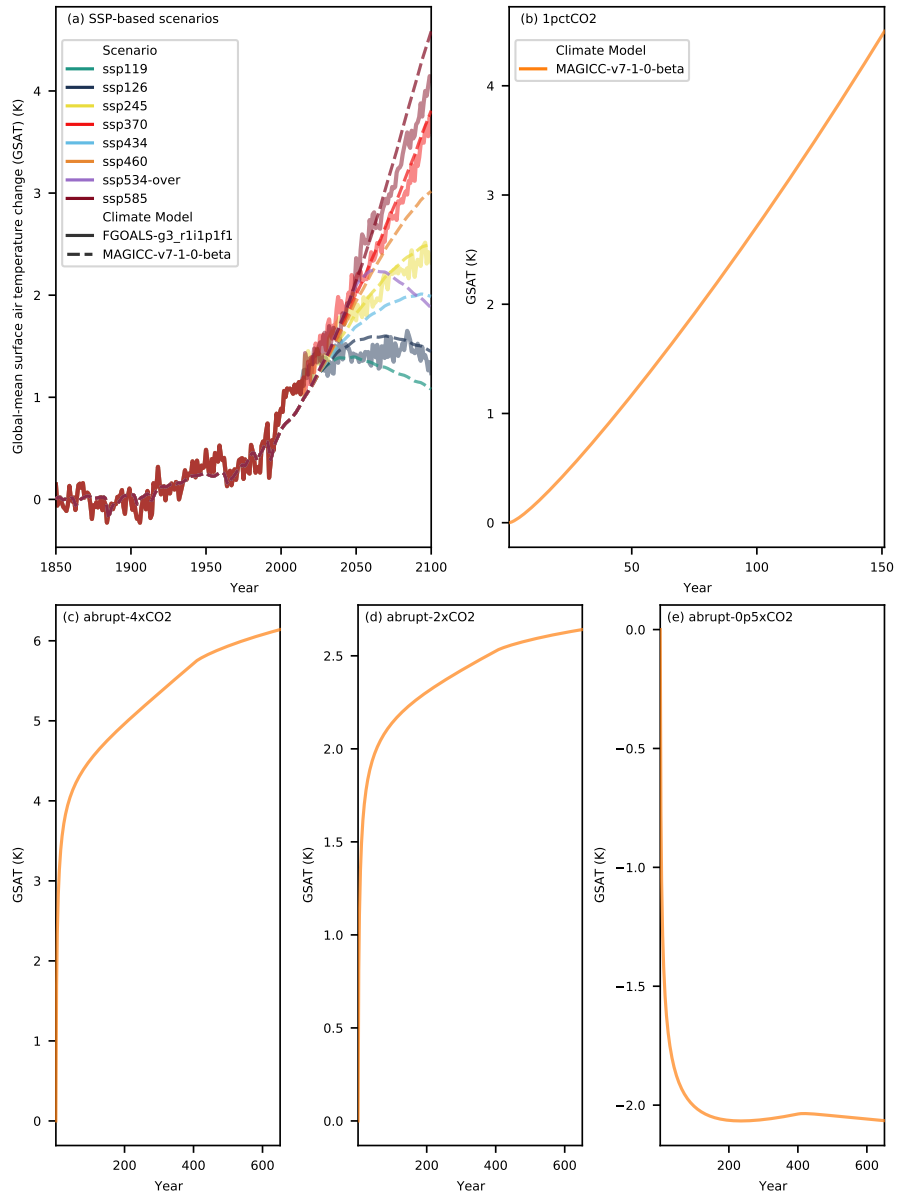


Figure S4. Emulation of FGOALS-g3_r1i1p1f1 by RCMs in RCMIP Phase 1. The thick transparent lines are the target CMIP6 model output (here from FGOALS-g3_r1i1p1f1). The thin lines are emulations from different RCMs. Panel (a) shows results for scenario based experiments while panels (b) - (e) show results for idealised CO₂-only experiments (note that panels (b) - (e) share the same legend).

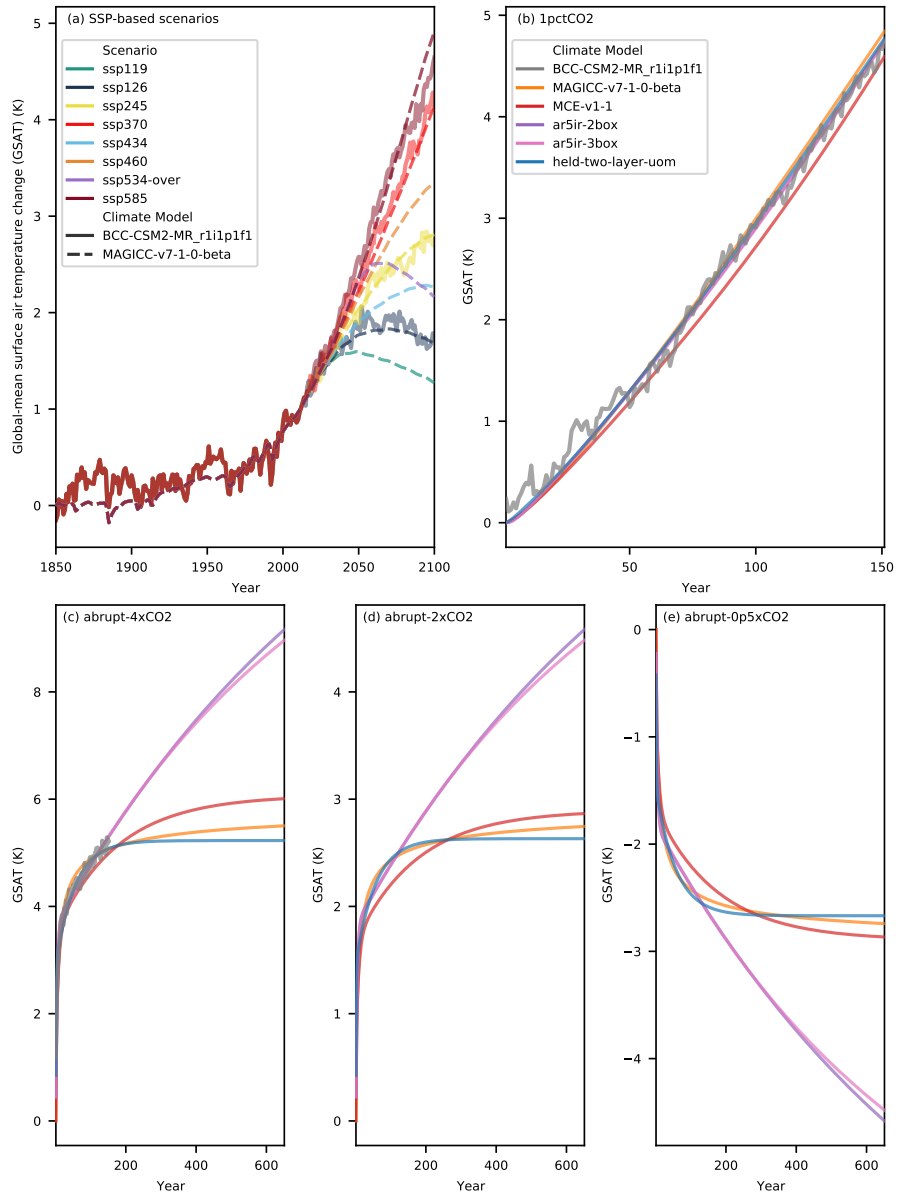


Figure S5. Emulation of BCC-CSM2-MR_r1i1p1f1 by RCMs in RCMIP Phase 1. The thick transparent lines are the target CMIP6 model output (here from BCC-CSM2-MR_r1i1p1f1). The thin lines are emulations from different RCMs. Panel (a) shows results for scenario based experiments while panels (b) - (e) show results for idealised CO₂-only experiments (note that panels (b) - (e) share the same legend).

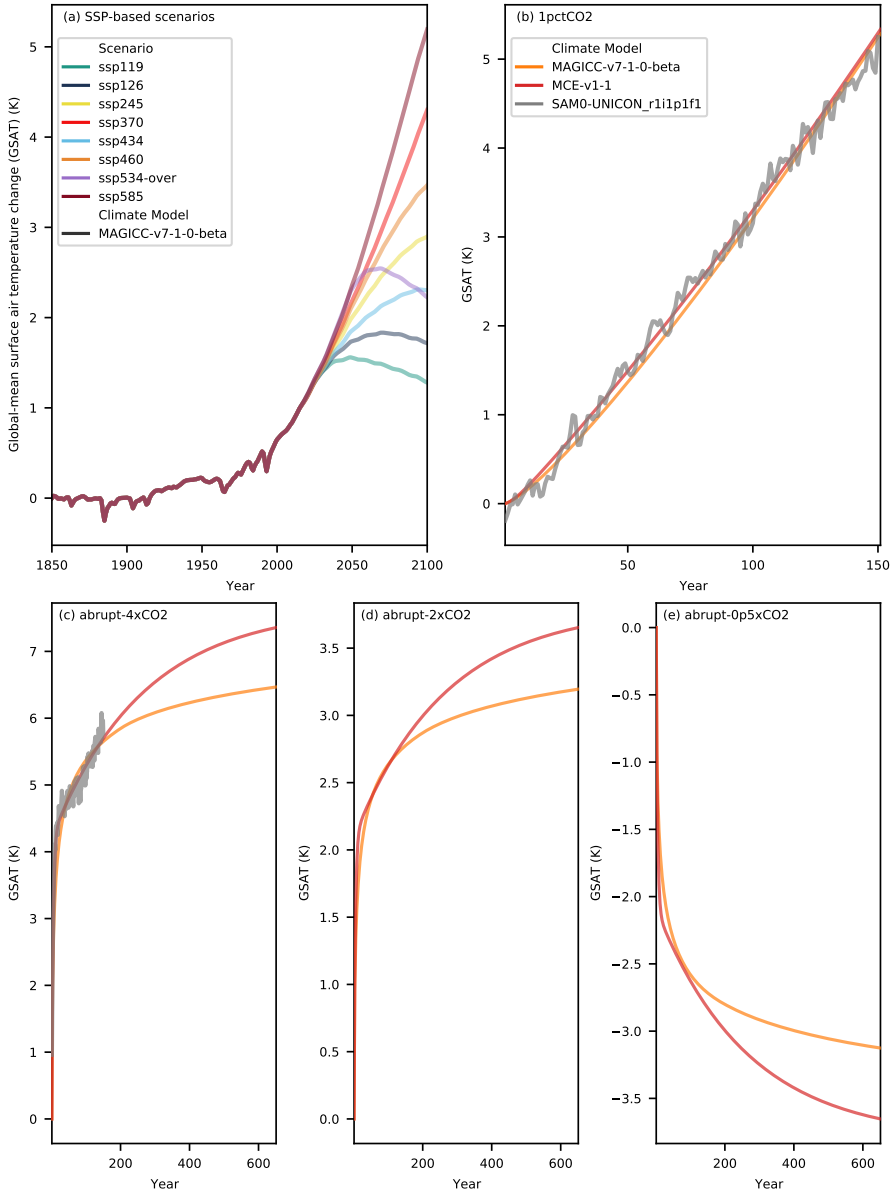


Figure S6. Emulation of SAM0-UNICON_r1i1p1f1 by RCMs in RCMIP Phase 1. The thick transparent lines are the target CMIP6 model output (here from SAM0-UNICON_r1i1p1f1). The thin lines are emulations from different RCMs. Panel (a) shows results for scenario based experiments while panels (b) - (e) show results for idealised CO₂-only experiments (note that panels (b) - (e) share the same legend).

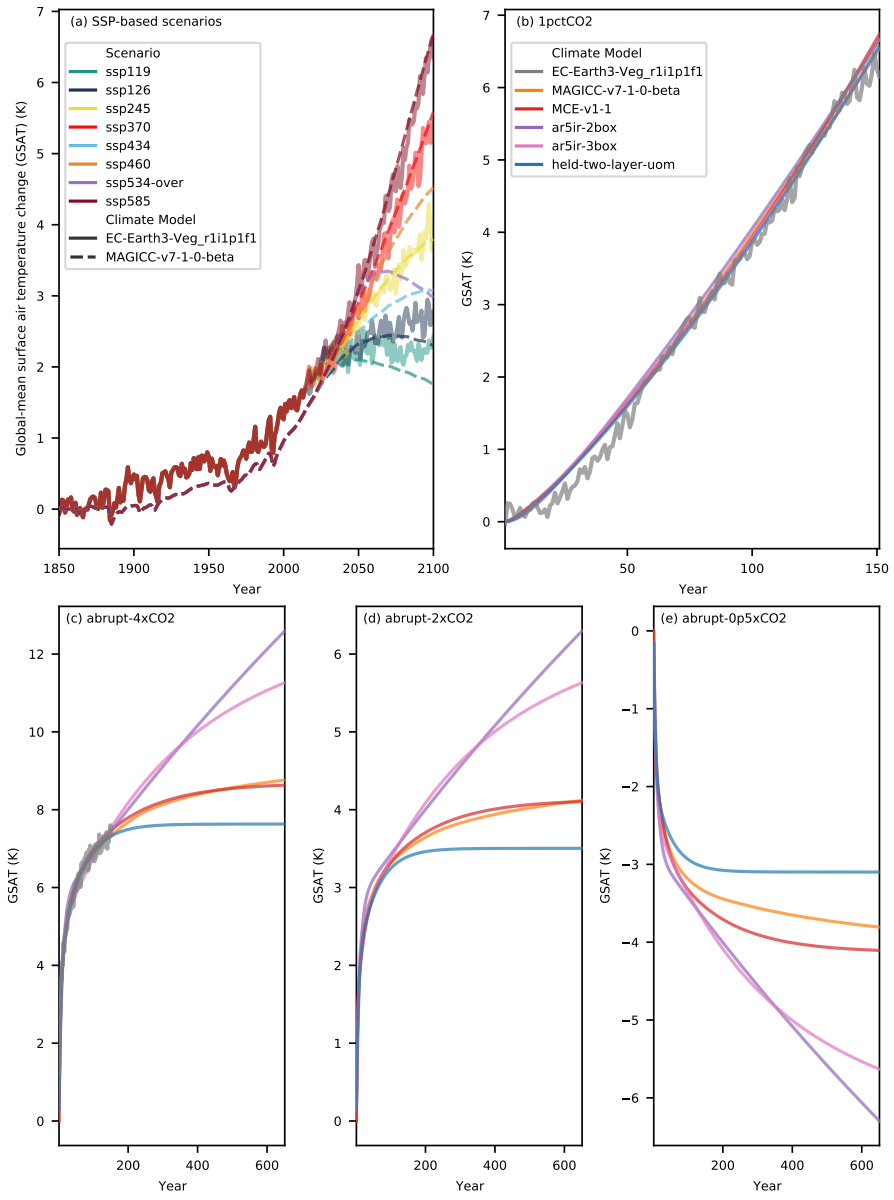


Figure S7. Emulation of EC-Earth3-Veg_r1i1p1f1 by RCMs in RCMIP Phase 1. The thick transparent lines are the target CMIP6 model output (here from EC-Earth3-Veg_r1i1p1f1). The thin lines are emulations from different RCMs. Panel (a) shows results for scenario based experiments while panels (b) - (e) show results for idealised CO₂-only experiments (note that panels (b) - (e) share the same legend).

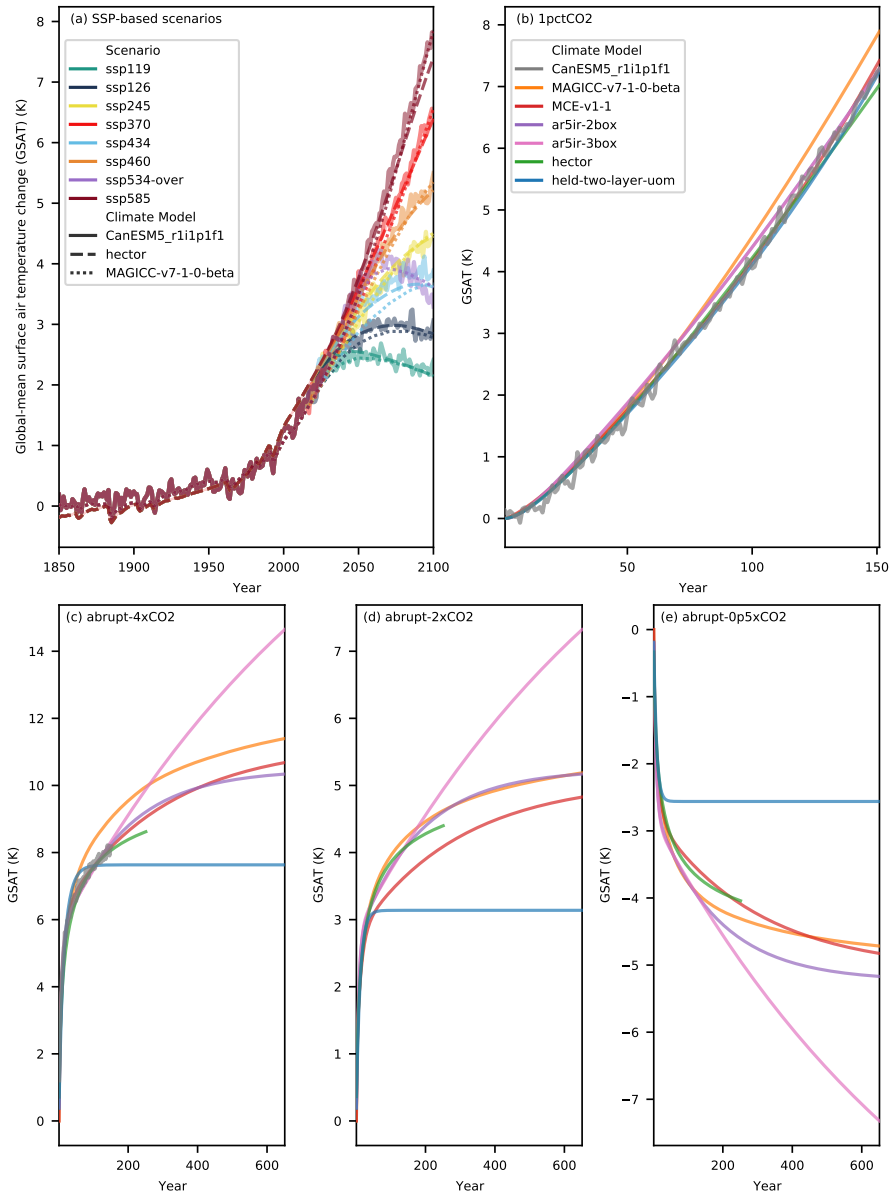


Figure S8. Emulation of CanESM5_r1i1p1f1 by RCMs in RCMIP Phase 1. The thick transparent lines are the target CMIP6 model output (here from CanESM5_r1i1p1f1). The thin lines are emulations from different RCMs. Panel (a) shows results for scenario based experiments while panels (b) - (e) show results for idealised CO₂-only experiments (note that panels (b) - (e) share the same legend).

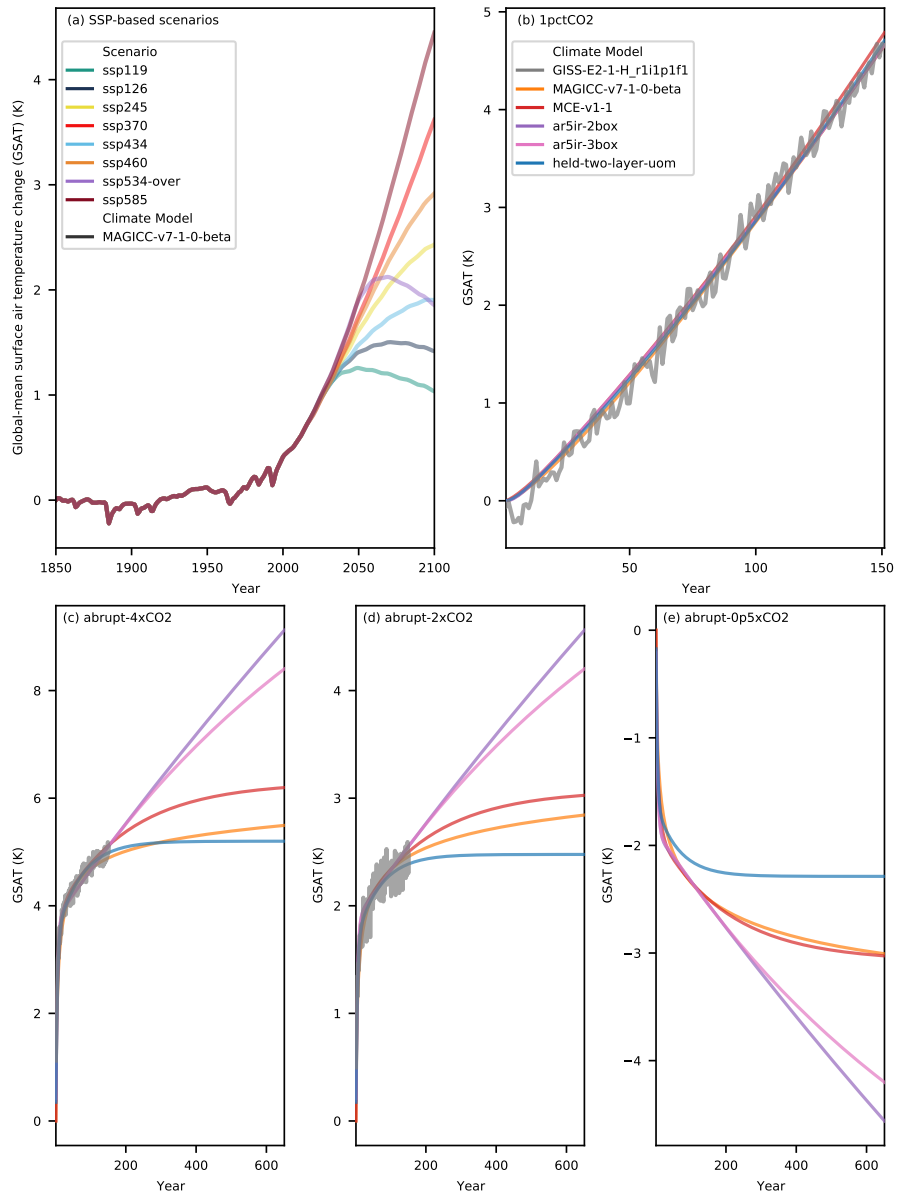


Figure S9. Emulation of GISS-E2-1-H_r1i1p1f1 by RCMs in RCMIP Phase 1. The thick transparent lines are the target CMIP6 model output (here from GISS-E2-1-H_r1i1p1f1). The thin lines are emulations from different RCMs. Panel (a) shows results for scenario based experiments while panels (b) - (e) show results for idealised CO₂-only experiments (note that panels (b) - (e) share the same legend).

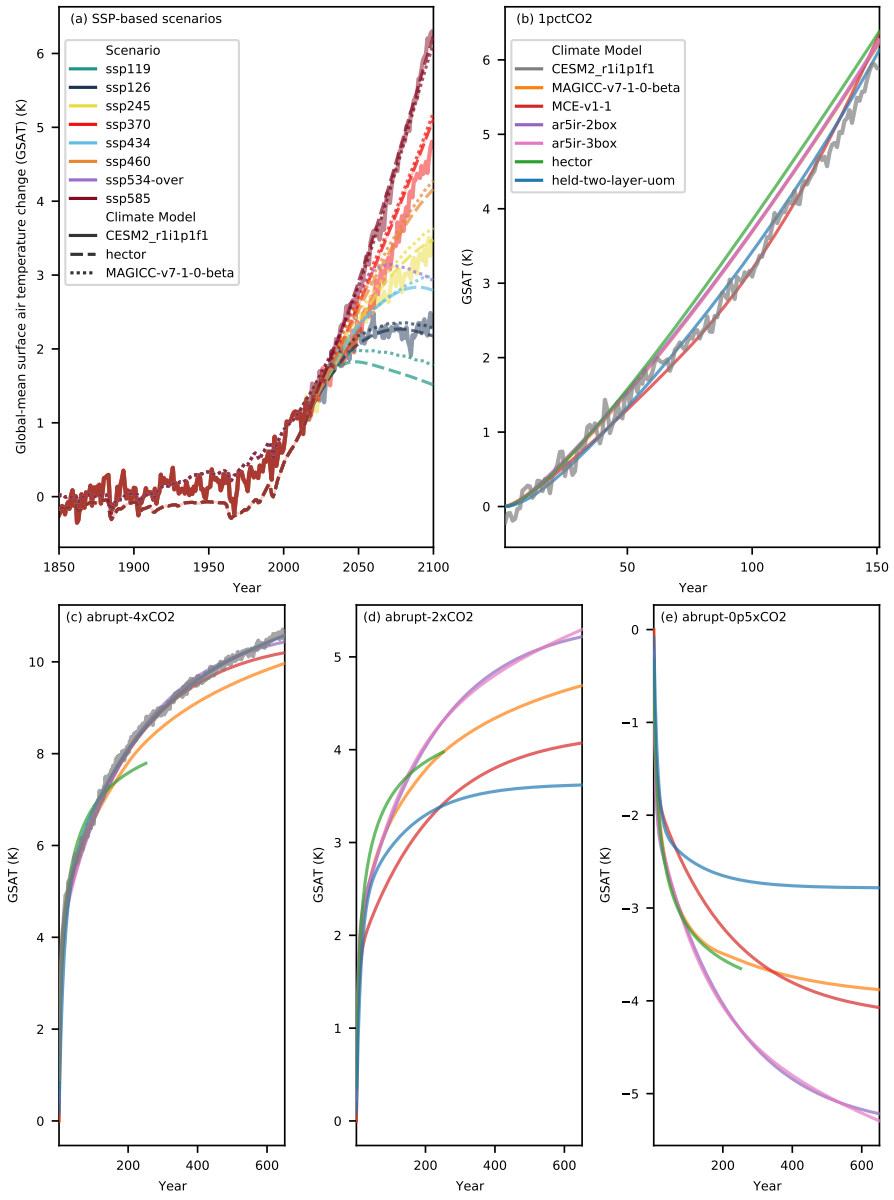


Figure S10. Emulation of CESM2_r1i1p1f1 by RCMs in RCMIP Phase 1. The thick transparent lines are the target CMIP6 model output (here from CESM2_r1i1p1f1). The thin lines are emulations from different RCMs. Panel (a) shows results for scenario based experiments while panels (b) - (e) show results for idealised CO₂-only experiments (note that panels (b) - (e) share the same legend).

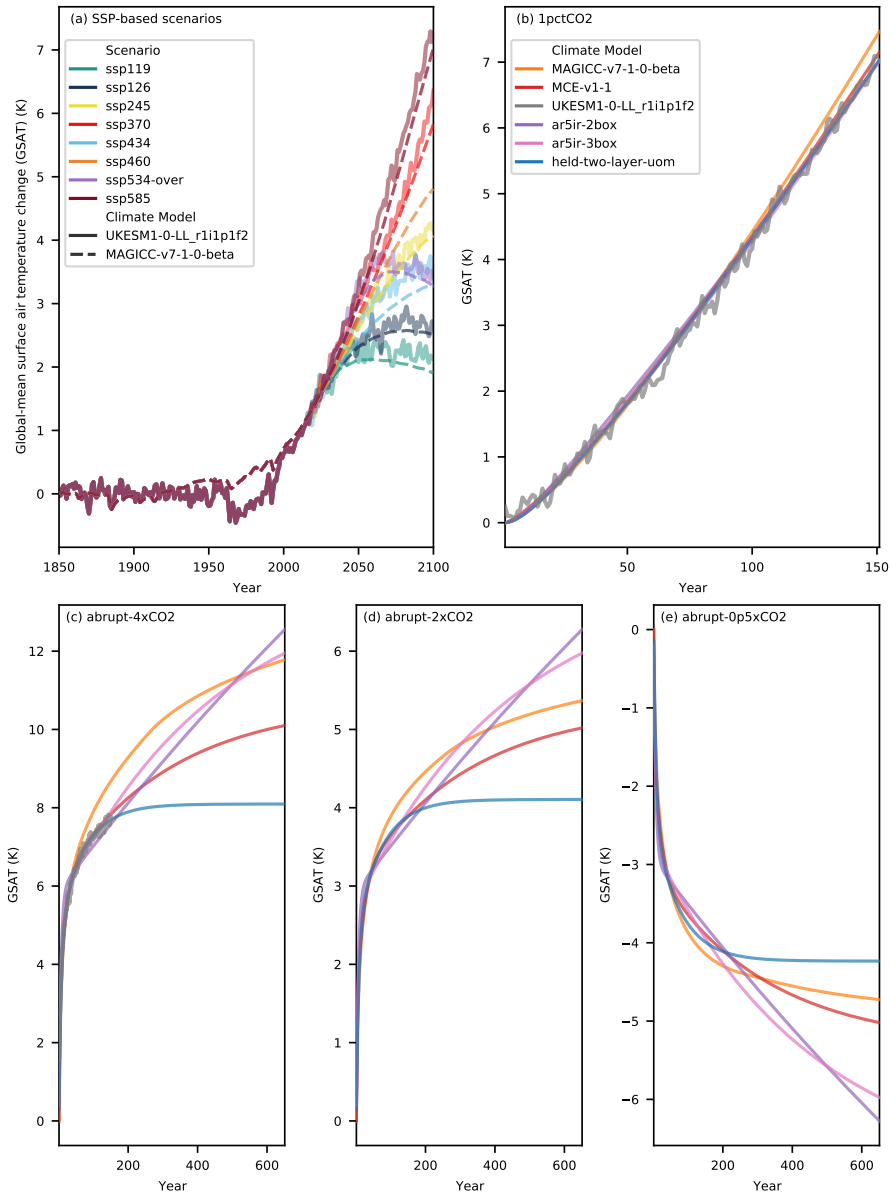


Figure S11. Emulation of UKESM1-0-LL_r1i1p1f2 by RCMs in RCMIP Phase 1. The thick transparent lines are the target CMIP6 model output (here from UKESM1-0-LL_r1i1p1f2). The thin lines are emulations from different RCMs. Panel (a) shows results for scenario based experiments while panels (b) - (e) show results for idealised CO₂-only experiments (note that panels (b) - (e) share the same legend).

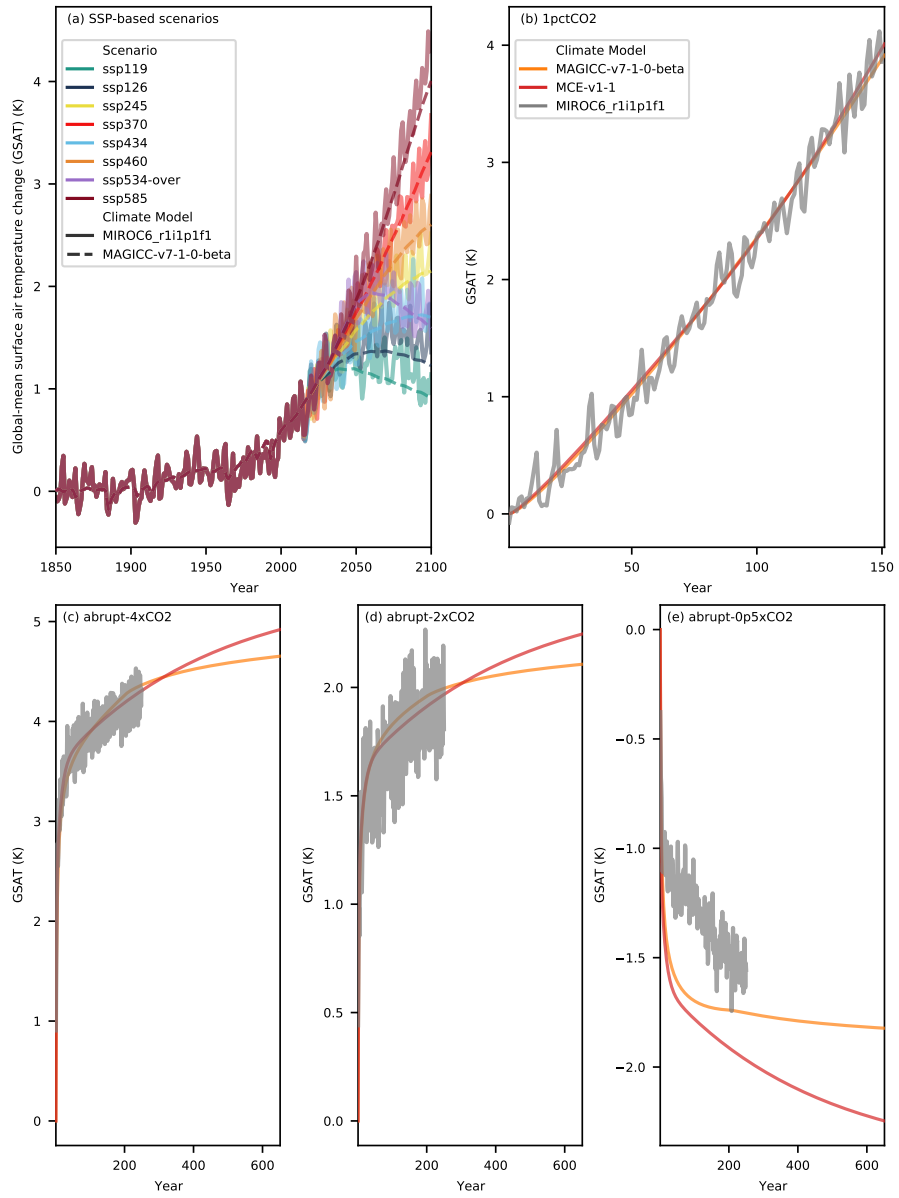


Figure S12. Emulation of MIROC6_r1i1p1f1 by RCMs in RCMIP Phase 1. The thick transparent lines are the target CMIP6 model output (here from MIROC6_r1i1p1f1). The thin lines are emulations from different RCMs. Panel (a) shows results for scenario based experiments while panels (b) - (e) show results for idealised CO₂-only experiments (note that panels (b) - (e) share the same legend).

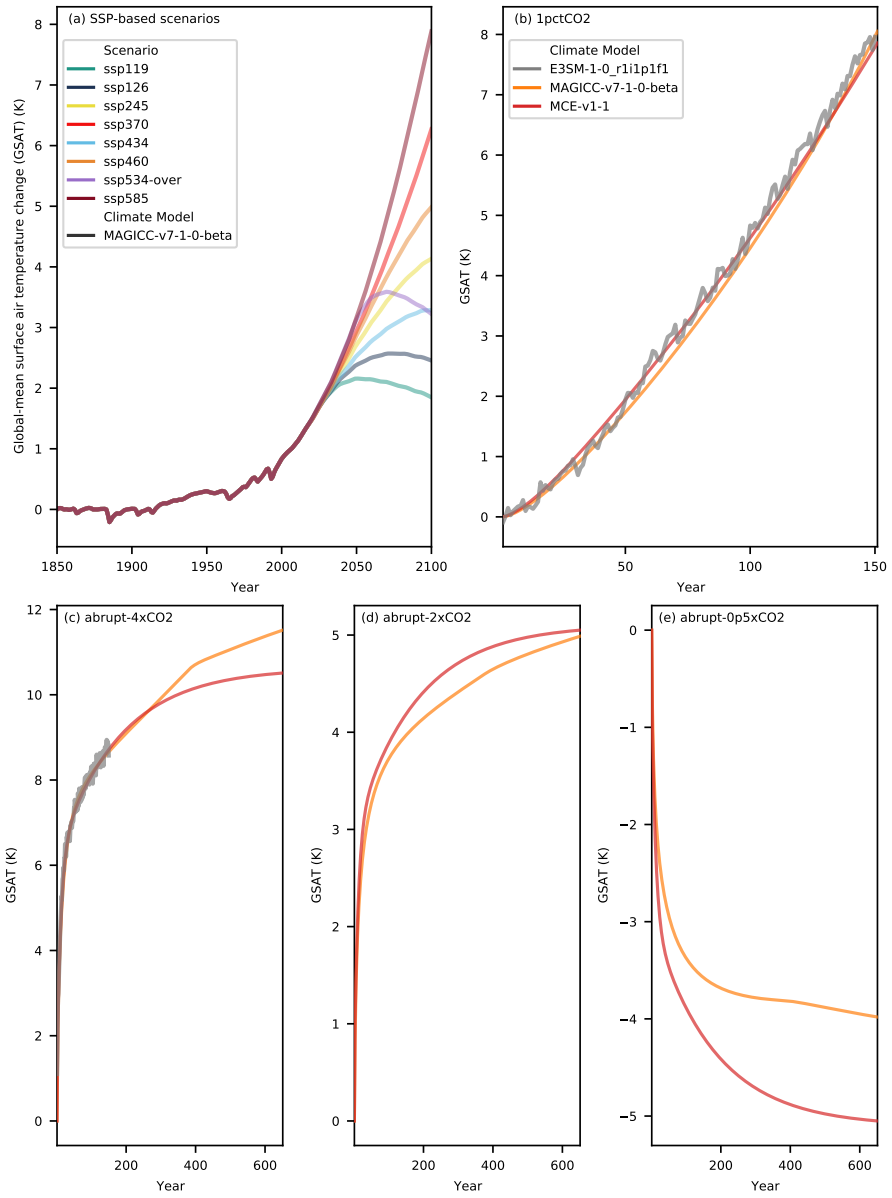


Figure S13. Emulation of E3SM-1-0_r1i1p1f1 by RCMs in RCMIP Phase 1. The thick transparent lines are the target CMIP6 model output (here from E3SM-1-0_r1i1p1f1). The thin lines are emulations from different RCMs. Panel (a) shows results for scenario based experiments while panels (b) - (e) show results for idealised CO₂-only experiments (note that panels (b) - (e) share the same legend).

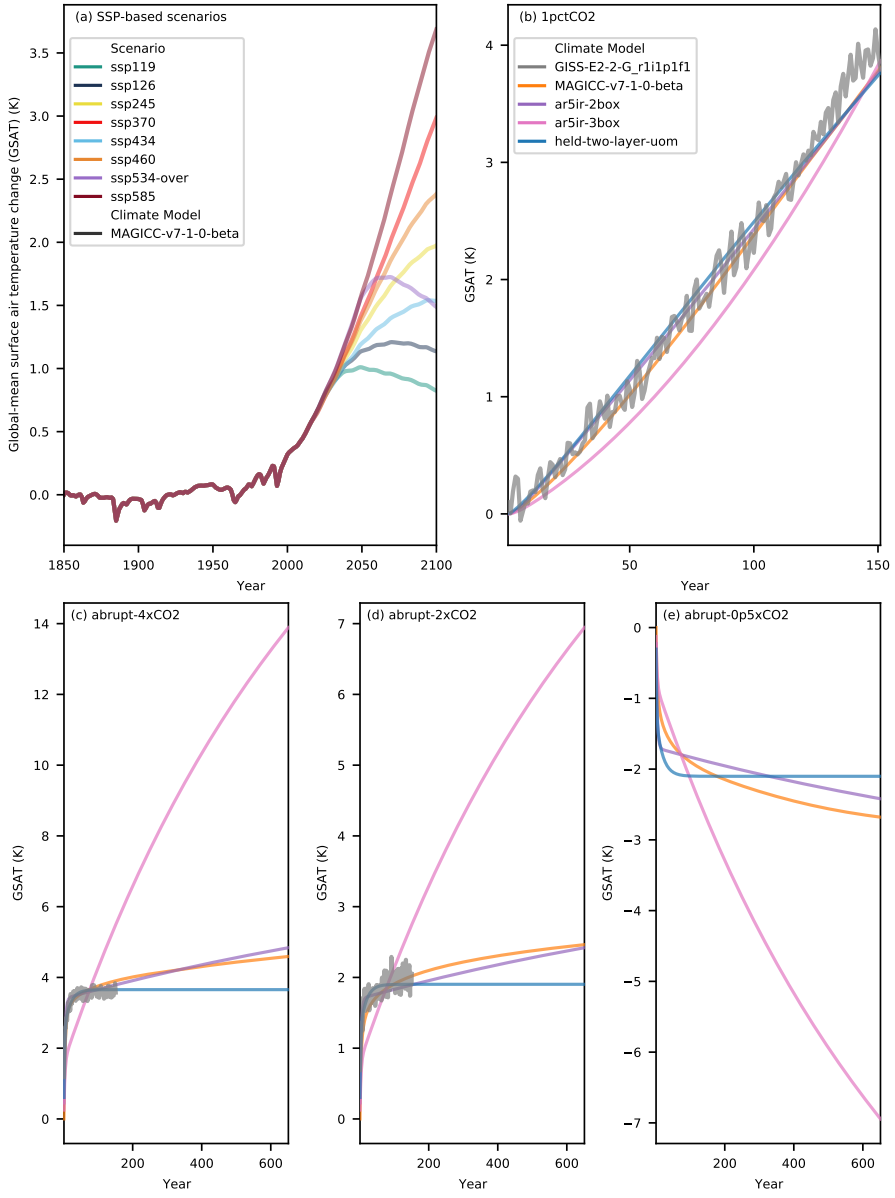


Figure S14. Emulation of GISS-E2-2-G_r1i1p1f1 by RCMs in RCMIP Phase 1. The thick transparent lines are the target CMIP6 model output (here from GISS-E2-2-G_r1i1p1f1). The thin lines are emulations from different RCMs. Panel (a) shows results for scenario based experiments while panels (b) - (e) show results for idealised CO₂-only experiments (note that panels (b) - (e) share the same legend).

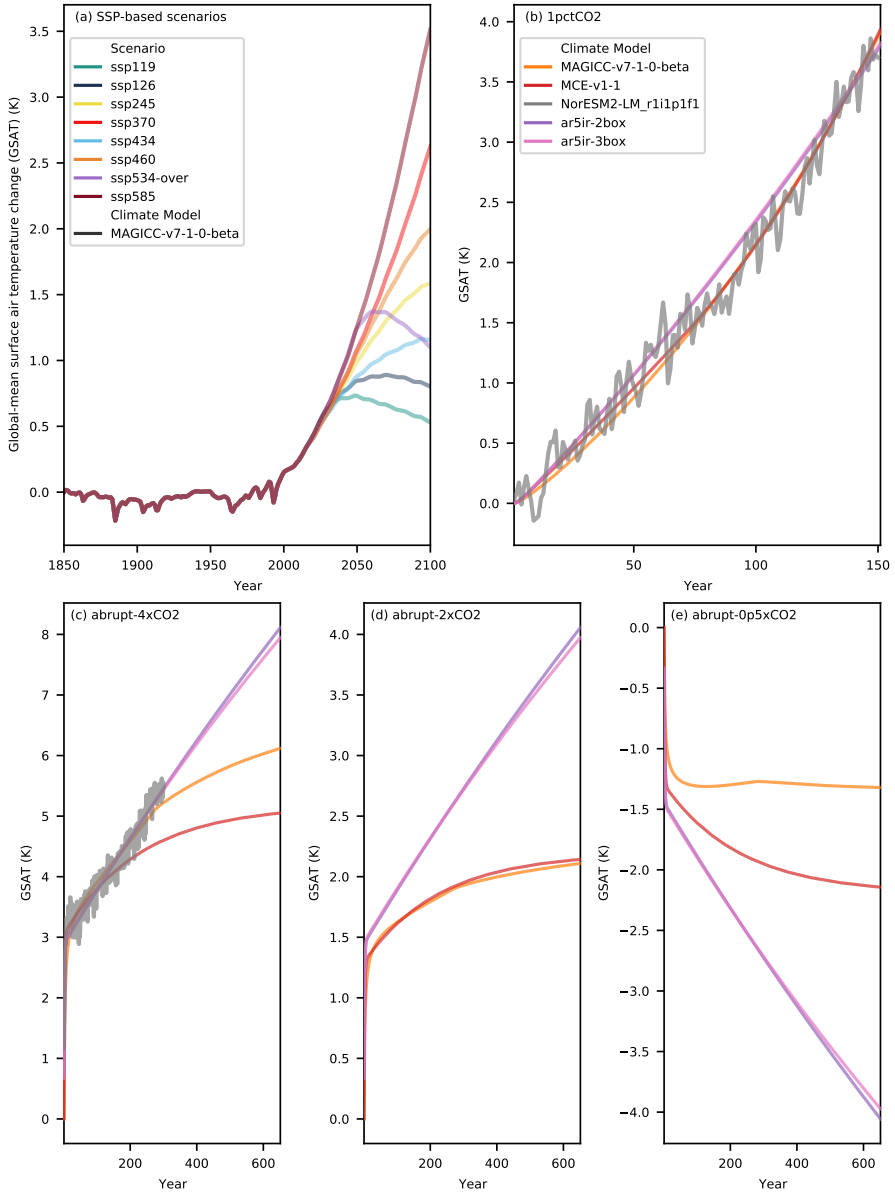


Figure S15. Emulation of NorESM2-LM_r1i1p1f1 by RCMs in RCMIP Phase 1. The thick transparent lines are the target CMIP6 model output (here from NorESM2-LM_r1i1p1f1). The thin lines are emulations from different RCMs. Panel (a) shows results for scenario based experiments while panels (b) - (e) show results for idealised CO₂-only experiments (note that panels (b) - (e) share the same legend).

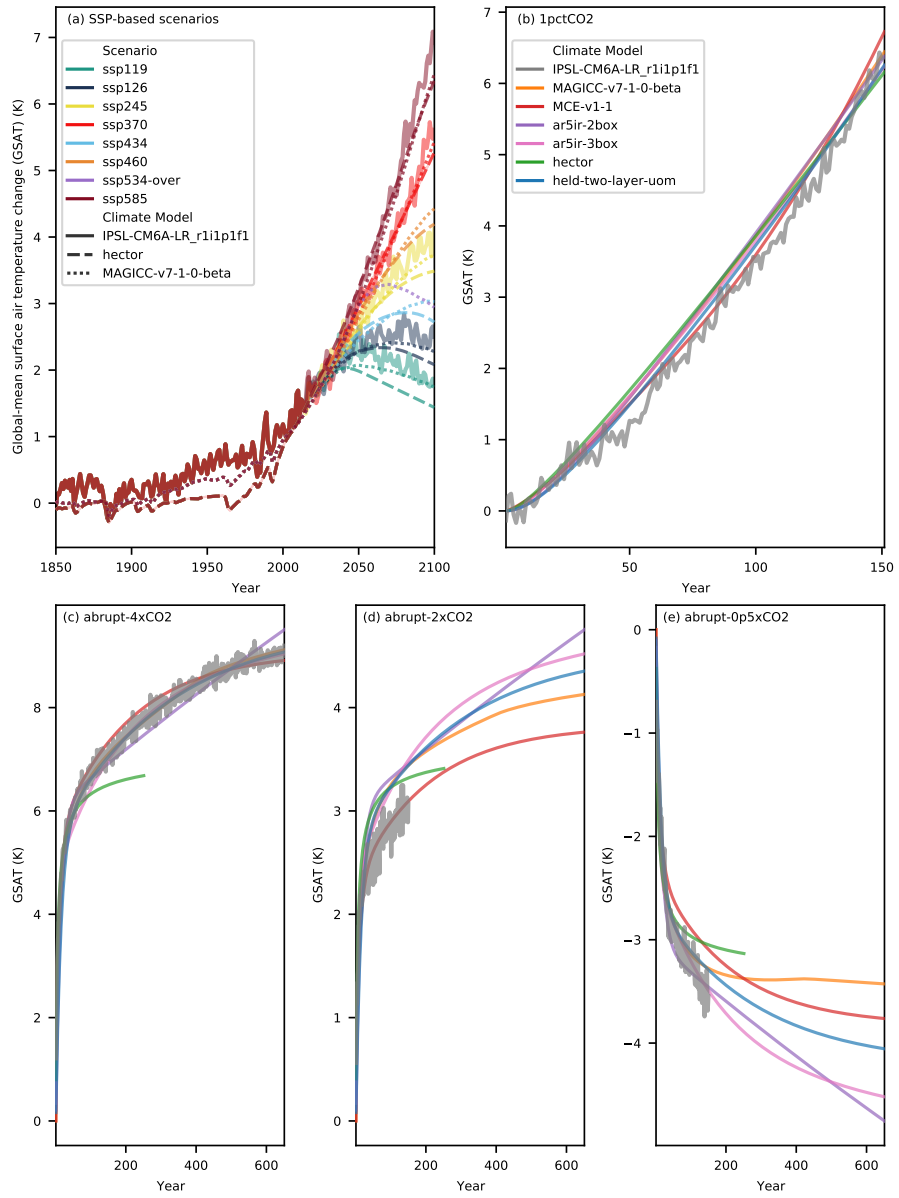


Figure S16. Emulation of IPSL-CM6A-LR_r1i1p1f1 by RCMs in RCMIP Phase 1. The thick transparent lines are the target CMIP6 model output (here from IPSL-CM6A-LR_r1i1p1f1). The thin lines are emulations from different RCMs. Panel (a) shows results for scenario based experiments while panels (b) - (e) show results for idealised CO₂-only experiments (note that panels (b) - (e) share the same legend).

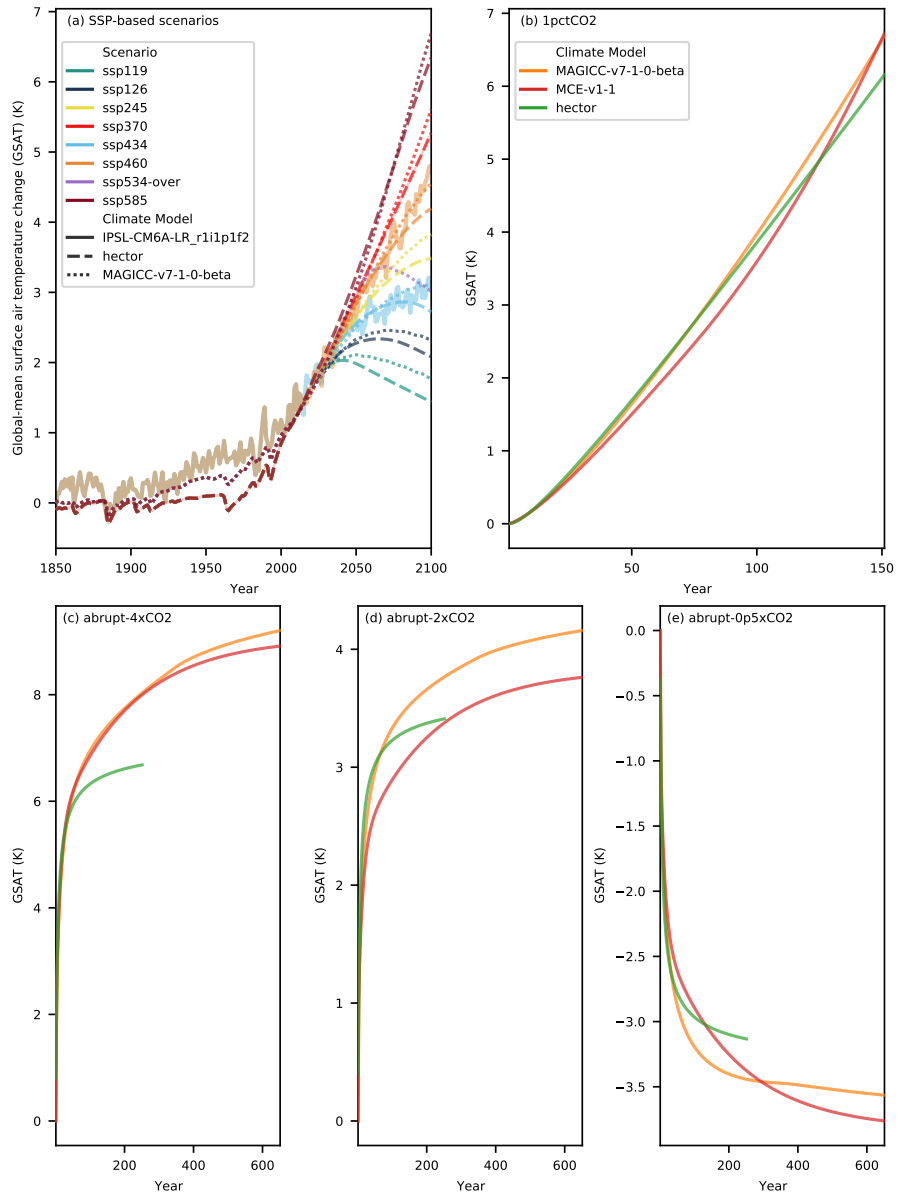


Figure S17. Emulation of IPSL-CM6A-LR_r1i1p1f2 by RCMs in RCMIP Phase 1. The thick transparent lines are the target CMIP6 model output (here from IPSL-CM6A-LR_r1i1p1f2). The thin lines are emulations from different RCMs. Panel (a) shows results for scenario based experiments while panels (b) - (e) show results for idealised CO₂-only experiments (note that panels (b) - (e) share the same legend).

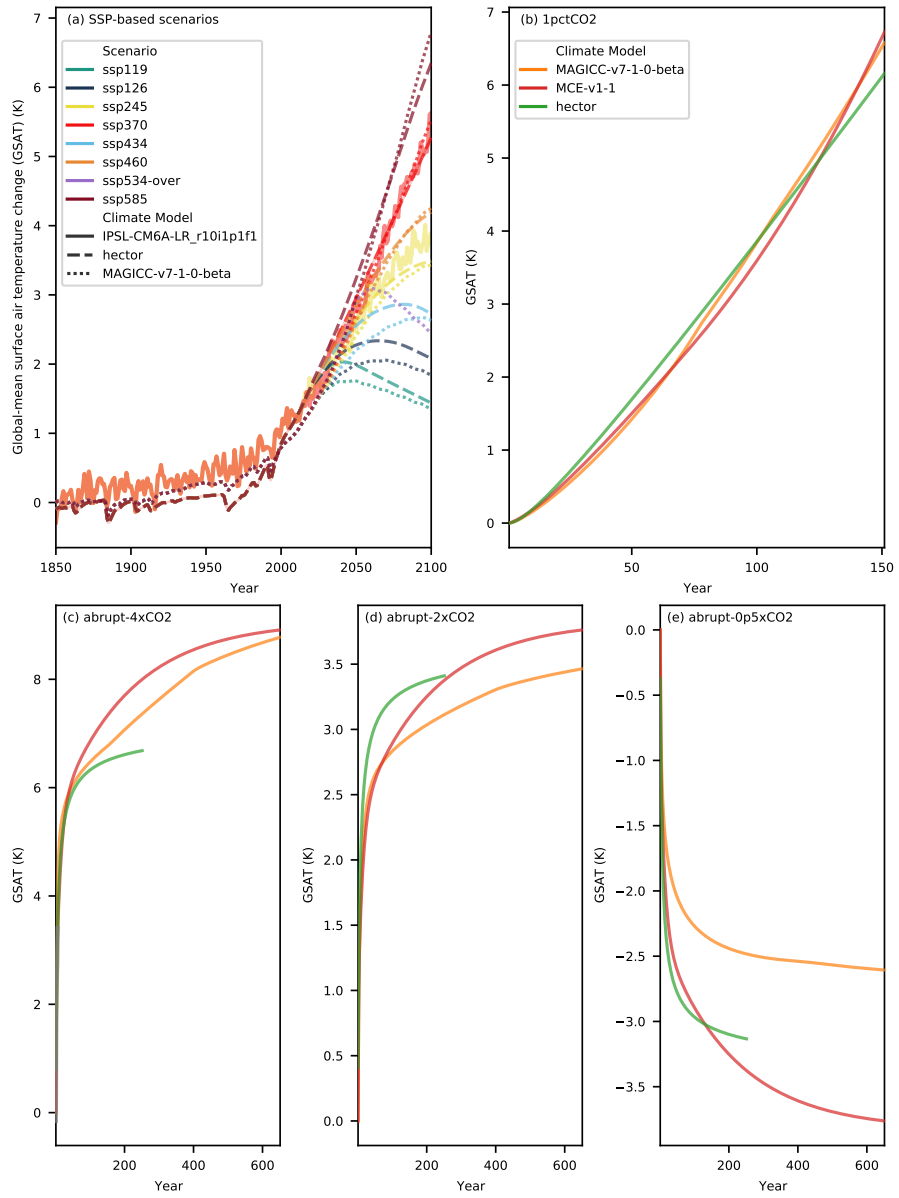


Figure S18. Emulation of IPSL-CM6A-LR_r10i1p1f1 by RCMs in RCMIP Phase 1. The thick transparent lines are the target CMIP6 model output (here from IPSL-CM6A-LR_r10i1p1f1). The thin lines are emulations from different RCMs. Panel (a) shows results for scenario based experiments while panels (b) - (e) show results for idealised CO₂-only experiments (note that panels (b) - (e) share the same legend).

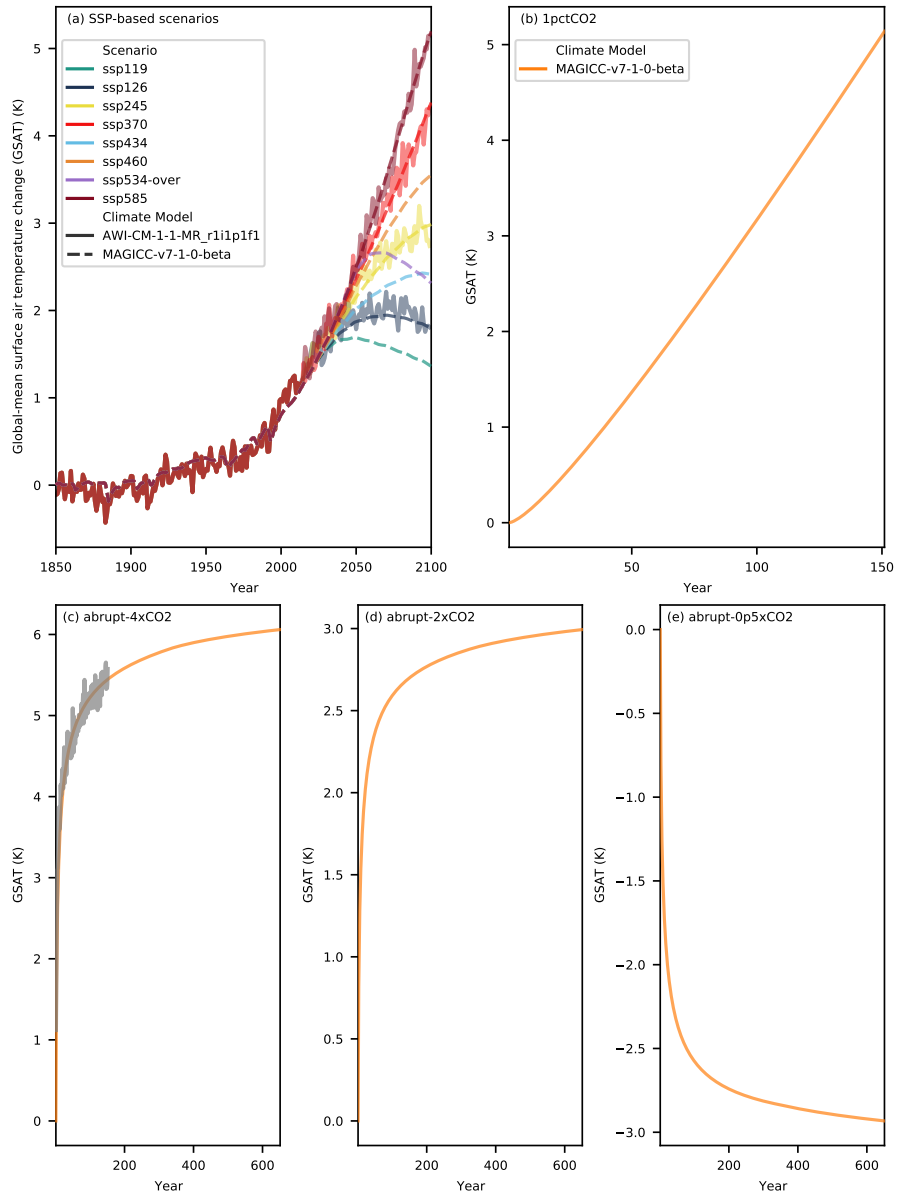


Figure S19. Emulation of AWI-CM-1-1-MR_r1i1p1f1 by RCMs in RCMIP Phase 1. The thick transparent lines are the target CMIP6 model output (here from AWI-CM-1-1-MR_r1i1p1f1). The thin lines are emulations from different RCMs. Panel (a) shows results for scenario based experiments while panels (b) - (e) show results for idealised CO₂-only experiments (note that panels (b) - (e) share the same legend).

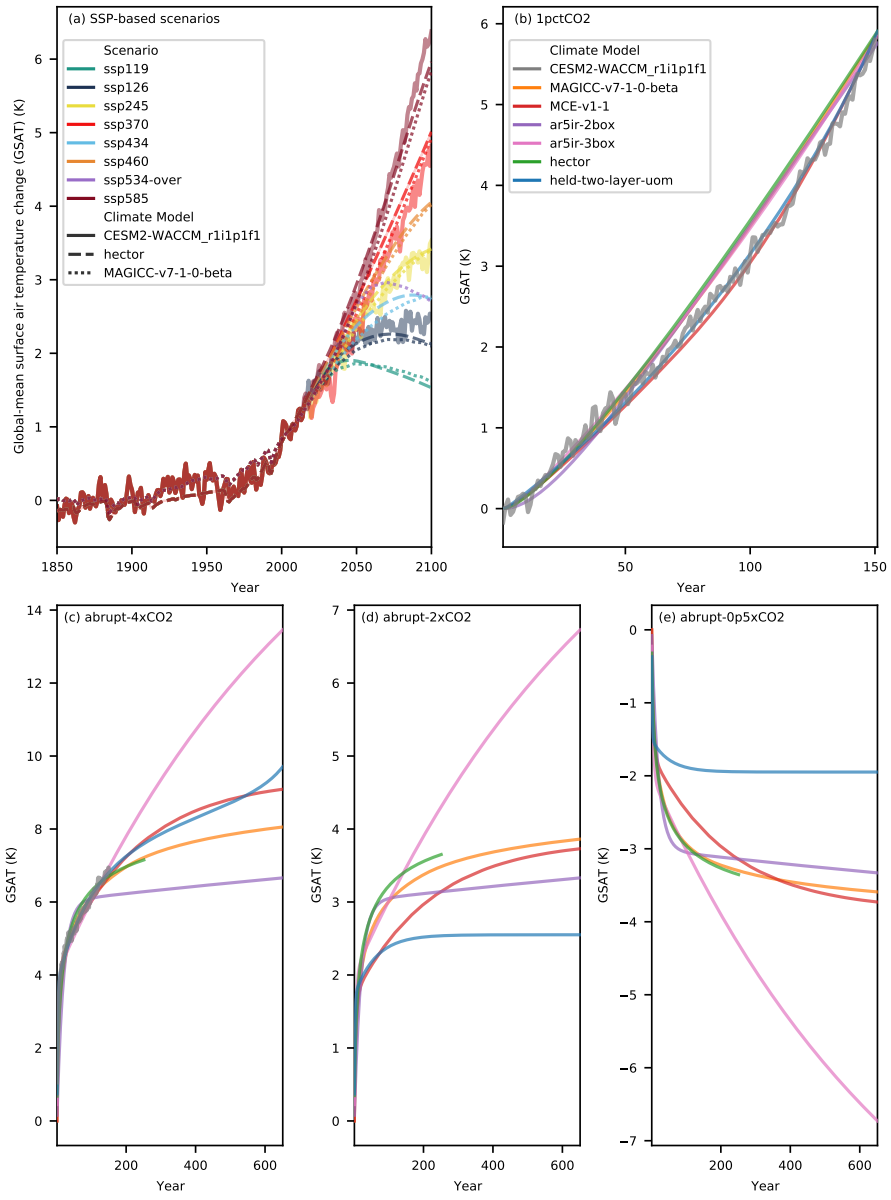


Figure S20. Emulation of CESM2-WACCM_r1i1p1f1 by RCMs in RCMIP Phase 1. The thick transparent lines are the target CMIP6 model output (here from CESM2-WACCM_r1i1p1f1). The thin lines are emulations from different RCMs. Panel (a) shows results for scenario based experiments while panels (b) - (e) show results for idealised CO₂-only experiments (note that panels (b) - (e) share the same legend).

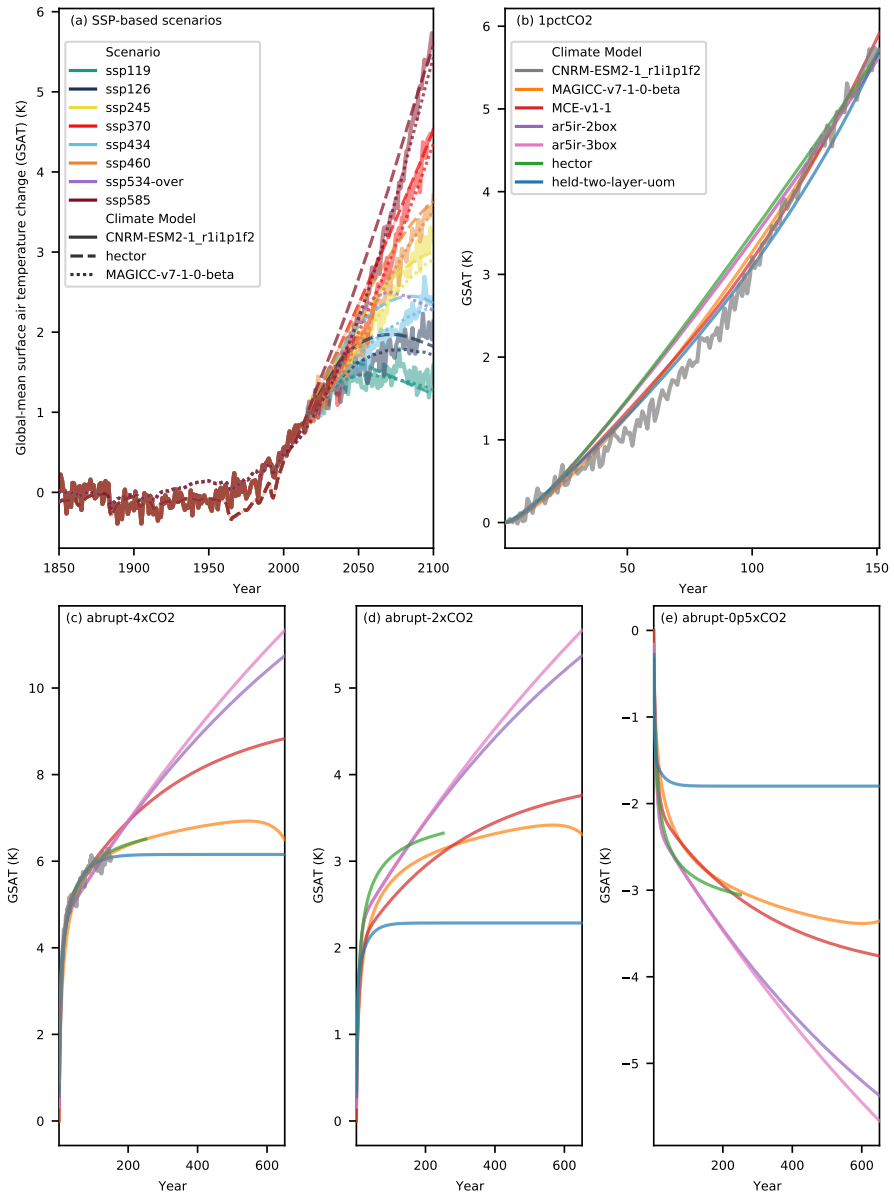


Figure S21. Emulation of CNRM-ESM2-1_r1i1p1f2 by RCMs in RCMIP Phase 1. The thick transparent lines are the target CMIP6 model output (here from CNRM-ESM2-1_r1i1p1f2). The thin lines are emulations from different RCMs. Panel (a) shows results for scenario based experiments while panels (b) - (e) show results for idealised CO₂-only experiments (note that panels (b) - (e) share the same legend).

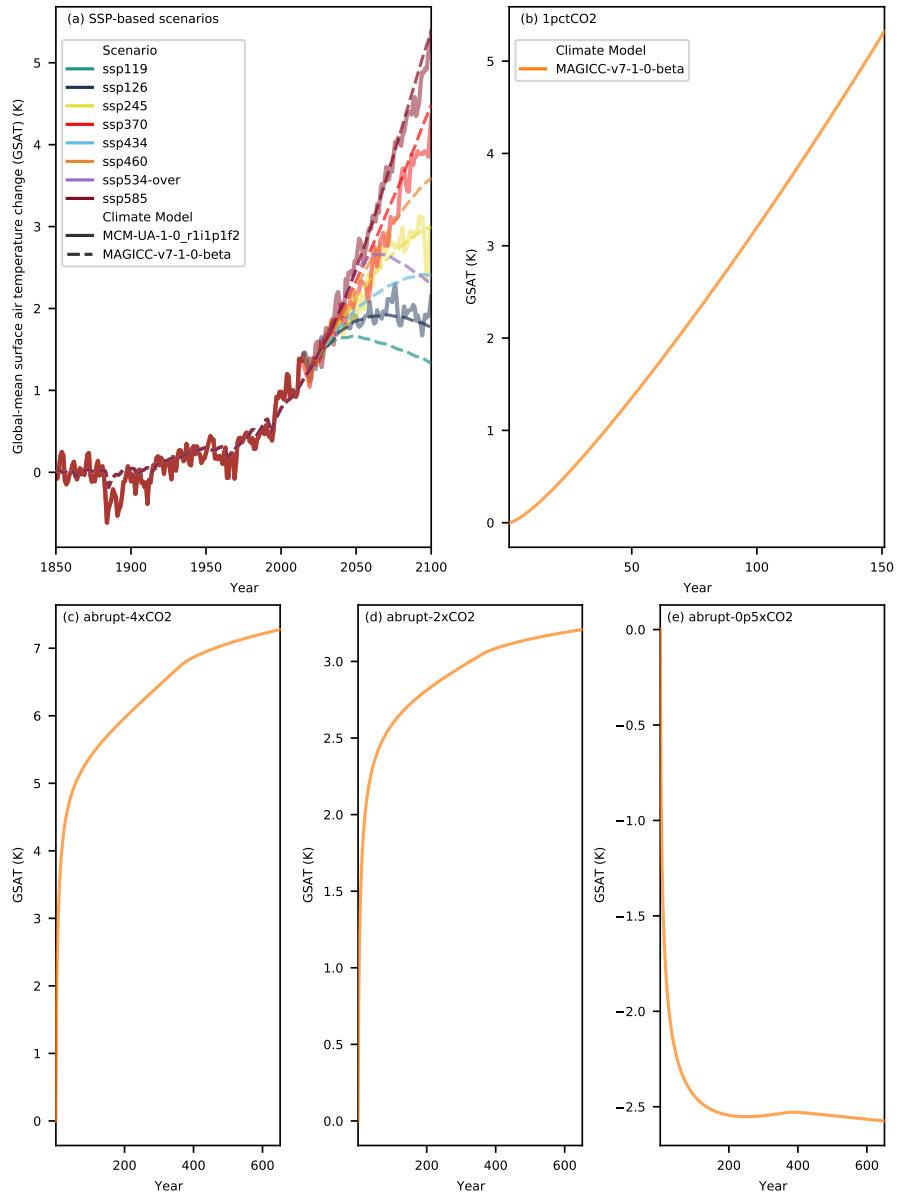


Figure S22. Emulation of MCM-UA-1-0_r1i1p1f2 by RCMs in RCMIP Phase 1. The thick transparent lines are the target CMIP6 model output (here from MCM-UA-1-0_r1i1p1f2). The thin lines are emulations from different RCMs. Panel (a) shows results for scenario based experiments while panels (b) - (e) show results for idealised CO₂-only experiments (note that panels (b) - (e) share the same legend).

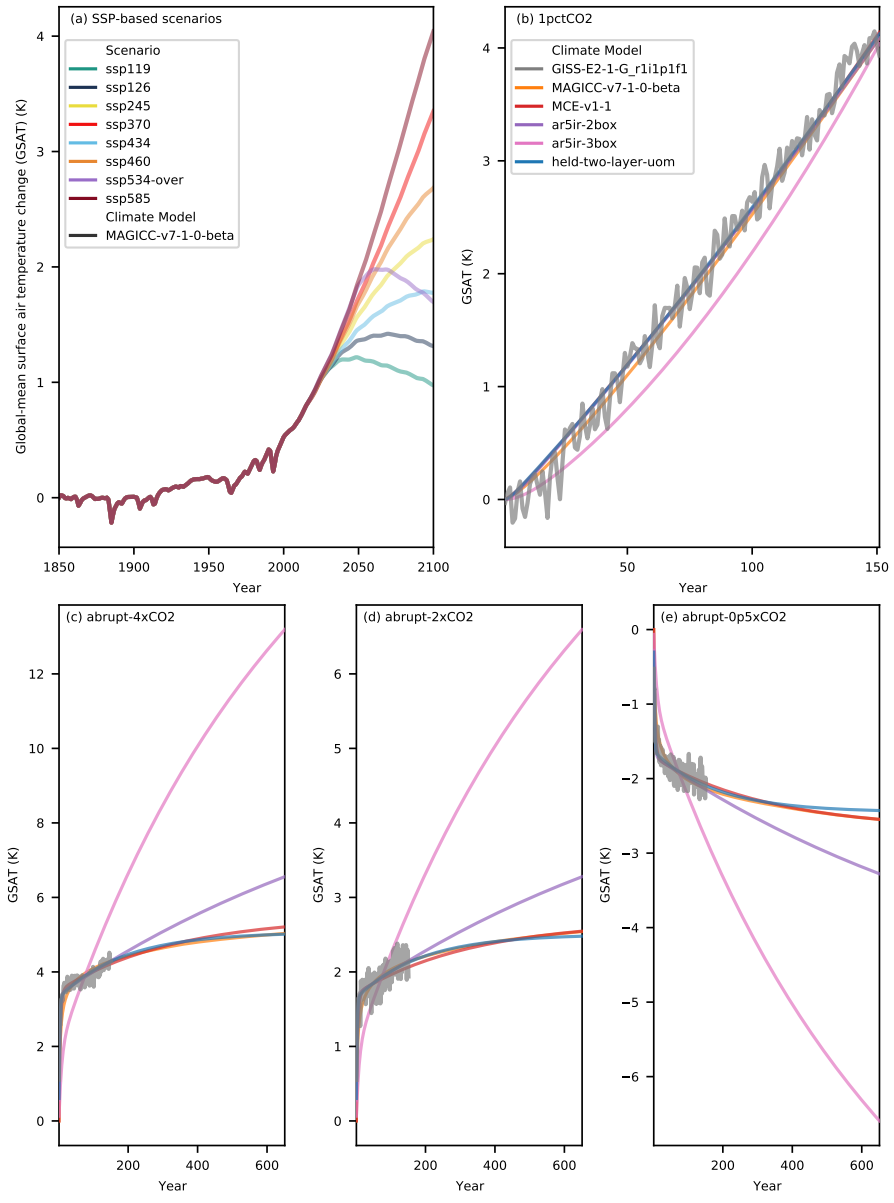


Figure S23. Emulation of GISS-E2-1-G_r1i1p1f1 by RCMs in RCMIP Phase 1. The thick transparent lines are the target CMIP6 model output (here from GISS-E2-1-G_r1i1p1f1). The thin lines are emulations from different RCMs. Panel (a) shows results for scenario based experiments while panels (b) - (e) show results for idealised CO₂-only experiments (note that panels (b) - (e) share the same legend).

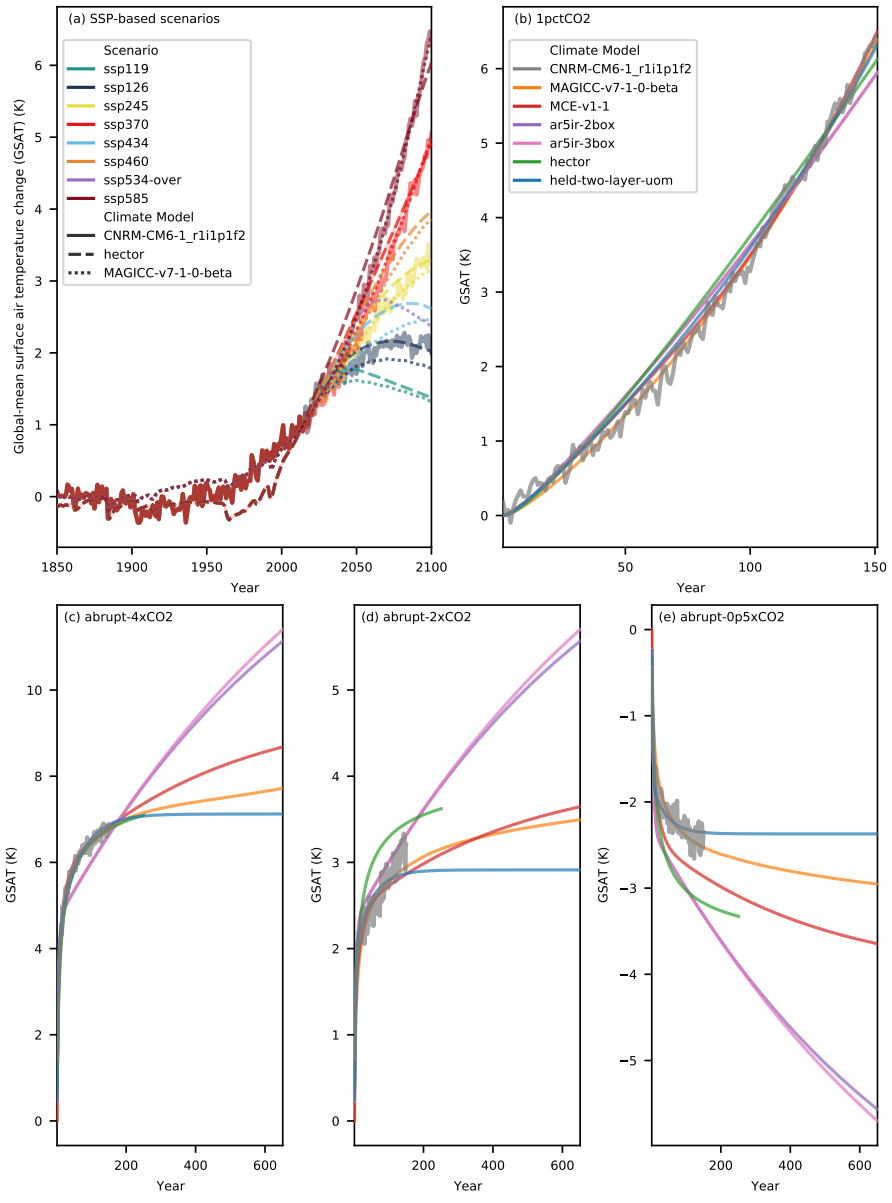


Figure S24. Emulation of CNRM-CM6-1_r1i1p1f2 by RCMs in RCMIP Phase 1. The thick transparent lines are the target CMIP6 model output (here from CNRM-CM6-1_r1i1p1f2). The thin lines are emulations from different RCMs. Panel (a) shows results for scenario based experiments while panels (b) - (e) show results for idealised CO₂-only experiments (note that panels (b) - (e) share the same legend).

Table S2. RCMIP Phase 1 variable overview (also available at rcmip.org).

| Variable | Unit | Definition |
|---|---------------------------------|--|
| Surface Air Temperature Change | K | Change in surface air temperature (i.e. 2m air temperature or best proxy thereof) |
| Effective Radiative Forcing | W m^{-2} | Effective radiative forcing from all anthropogenic and natural sources (after stratospheric temperature adjustments and rapid adjustments) |
| Effective Radiative Forcing Anthropogenic Aerosols | W m^{-2} | Effective radiative forcing from aerosols (after stratospheric temperature adjustments and rapid adjustments) |
| Effective Radiative Forcing Anthropogenic CO ₂ | W m^{-2} | Effective radiative forcing (after stratospheric temperature adjustments and rapid adjustments) of CO ₂ |
| Emissions CO ₂ | $\text{MtCO}_2 \text{ yr}^{-1}$ | Total carbon dioxide emissions |

References

Gidden, M. and Huppmann, D.: pyam: a Python Package for the Analysis and Visualization of Models of the Interaction of Climate, Human, and Environmental Systems, *Journal of Open Source Software*, 4, 1095, <https://doi.org/10.21105/joss.01095>, 2019.

Gidden, M. J., Riahi, K., Smith, S. J., Fujimori, S., Luderer, G., Kriegler, E., van Vuuren, D. P., van den Berg, M., Feng, L., Klein, D., Calvin, 65
K., Doelman, J. C., Frank, S., Fricko, O., Harmsen, M., Hasegawa, T., Havlik, P., Hilaire, J., Hoesly, R., Horing, J., Popp, A., Stehfest, E., and Takahashi, K.: Global emissions pathways under different socioeconomic scenarios for use in CMIP6: a dataset of harmonized emissions trajectories through the end of the century, *Geoscientific Model Development*, 12, 1443–1475, <https://doi.org/10.5194/gmd-12-1443-2019>, 2019.

Gütschow, J., Jeffery, M. L., Gieseke, R., Gebel, R., Stevens, D., Krapp, M., and Rocha, M.: The PRIMAP-hist national historical emissions 70
time series, *Earth System Science Data*, 8, 571–603, <https://doi.org/10.5194/essd-8-571-2016>, 2016.

Harmsen, M. J. H. M., van Vuuren, D. P., van den Berg, M., Hof, A. F., Hope, C., Krey, V., Lamarque, J.-F., Marcucci, A., Shindell, D. T., and Schaeffer, M.: How well do integrated assessment models represent non-CO₂ radiative forcing?, *Climatic Change*, 133, 565–582, <https://doi.org/10.1007/s10584-015-1485-0>, 2015.

Hoesly, R. M., Smith, S. J., Feng, L., Klimont, Z., Janssens-Maenhout, G., Pitkanen, T., Seibert, J. J., Vu, L., Andres, R. J., Bolt, R. M., Bond, 75
T. C., Dawidowski, L., Kholod, N., Kurokawa, J.-i., Li, M., Liu, L., Lu, Z., Moura, M. C. P., O'Rourke, P. R., and Zhang, Q.: Historical (1750–2014) anthropogenic emissions of reactive gases and aerosols from the Community Emissions Data System (CEDS), *Geoscientific Model Development*, 11, 369–408, <https://doi.org/10.5194/gmd-11-369-2018>, 2018.

Houghton, J. T., Meira Filho, L. G., Griggs, D. J., and Maskell, K.: An introduction to simple climate models used in the IPCC Second Assessment Report, Cambridge University Press Cambridge, <http://large.stanford.edu/courses/2015/ph240/girard1/docs/houghton.pdf>, 1997.

Meinshausen, M., Smith, S. J., Calvin, K., Daniel, J. S., Kainuma, M. L. T., Lamarque, J.-F., Matsumoto, K., Montzka, S. A., Raper, S. C. B., 80
Riahi, K., Thomson, A., Velders, G. J. M., and van Vuuren, D. P.: The RCP greenhouse gas concentrations and their extensions from 1765 to 2300, *Climatic Change*, 109, 213–241, <https://doi.org/10.1007/s10584-011-0156-z>, 2011.

Meinshausen, M., Nicholls, Z. R. J., Lewis, J., Gidden, M. J., Vogel, E., Freund, M., Beyerle, U., Gessner, C., Nauels, A., Bauer, N., Canadell, J. G., Daniel, J. S., John, A., Krummel, P. B., Luderer, G., Meinshausen, N., Montzka, S. A., Rayner, P. J., Reimann, S., Smith, 85
S. J., van den Berg, M., Velders, G. J. M., Vollmer, M. K., and Wang, R. H. J.: The shared socio-economic pathway (SSP) greenhouse gas concentrations and their extensions to 2500, *Geoscientific Model Development*, 13, 3571–3605, <https://doi.org/10.5194/gmd-13-3571-2020>, <https://gmd.copernicus.org/articles/13/3571/2020/>, 2020.

Quéré, C. L., Andrew, R. M., Canadell, J. G., Sitch, S., Korsbakken, J. I., Peters, G. P., Manning, A. C., Boden, T. A., Tans, P. P., Houghton, 90
R. A., Keeling, R. F., Alin, S., Andrews, O. D., Anthoni, P., Barbero, L., Bopp, L., Chevallier, F., Chini, L. P., Ciais, P., Currie, K., Delire, C., Doney, S. C., Friedlingstein, P., Gkriztalis, T., Harris, I., Hauck, J., Haverd, V., Hoppe, M., Goldewijk, K. K., Jain, A. K., Kato, E., Körtzinger, A., Landschützer, P., Lefèvre, N., Lenton, A., Lienert, S., Lombardozzi, D., Melton, J. R., Metzl, N., Millero, F., Monteiro, P. P. M. S., Munro, D. R., Nabel, J. E. M. S., Nakaoka, S.-i., O'Brien, K., Olsen, A., Omar, A. M., Ono, T., Pierrot, D., Poulter, B., Rödenbeck, C., Salisbury, J., Schuster, U., Schwinger, J., Séférian, R., Skjelvan, I., Stocker, B. D., Sutton, A. J., Takahashi, T., Tian, H., Tilbrook, B., van der Laan-Luijkx, I. T., van der Werf, G. R., Viovy, N., Walker, A. P., Wiltshire, A. J., and Zaehle, S.: Global Carbon Budget 2016, 95
Earth System Science Data, 8, 605–649, <https://doi.org/10.5194/essd-8-605-2016>, 2016.

Schwarber, A. K., Smith, S. J., Hartin, C. A., Vega-Westhoff, B. A., and Srivastava, R.: Evaluating climate emulation: fundamental impulse testing of simple climate models, *Earth System Dynamics*, 10, 729–739, <https://doi.org/10.5194/esd-10-729-2019>, 2019.

- van Marle, M. J. E., Kloster, S., Magi, B. I., Marlon, J. R., Daniau, A.-L., Field, R. D., Arneth, A., Forrest, M., Hantson, S., Kehrwald, N. M., Knorr, W., Lasslop, G., Li, F., Mangeon, S., Yue, C., Kaiser, J. W., and van der Werf, G. R.: Historic global biomass burning emissions for
100 CMIP6 (BB4CMIP) based on merging satellite observations with proxies and fire models (1750–2015), Geoscientific Model Development, 10, 3329–3357, <https://doi.org/10.5194/gmd-10-3329-2017>, 2017.
- van Vuuren, D. P., Lowe, J., Stehfest, E., Gohar, L., Hof, A. F., Hope, C., Warren, R., Meinshausen, M., and Plattner, G.-K.: How well do integrated assessment models simulate climate change?, Climatic Change, 104, 255–285, <https://doi.org/10.1007/s10584-009-9764-2>, 2011.
- 105 Wickham, H.: Tidy Data, Journal of Statistical Software, Articles, 59, 1–23, <https://doi.org/10.18637/jss.v059.i10>, <https://www.jstatsoft.org/v059/i10>, 2014.